OREGON STATE UNIVERSITY, COLLEGE OF CIVIL AND CONSTRUCTION ENGINEERING

Design and Construction of a Real-time Ocean Mooring at Strawberry Hill

Masters of Science Project Report

Daniel E. Lutz

12/10/2008

Master of Science technical report of Daniel E. Lutz presented on November 24, 2008

APPROVED:

Merrick C. Haller, Major Professor, representing Civil Engineering

Scott A. Ashford, Head of the Department of Civil and Construction Engineering

I understand that my technical report will become part of the permanent collection of Oregon State University libraries. My signature below authorizes release of my project to any reader upon request.

Daniel E. Lutz, Author

Table of Contents

List of Equations

List of Figures

List of Tables

1 Abstract

"Design and Construction of a Real-time Ocean Mooring at Strawberry Hill" (2008), demonstrates a sound design for an oceanographic mooring on the Oregon Coast. The purpose of the real-time mooring is to collect dissolved oxygen data for the determination of hypoxic areas, and to transmit the data on demand to researchers via a cell phone modem. The real-time mooring was successfully deployed for one week in September 2008. Then the mooring was analyzed numerically to determine its static and dynamic response in extreme site conditions and its potential modes of failure. This project is an interdisciplinary partnership between the Coastal and Ocean Engineering Program and the researchers in the Partnership for Interdisciplinary Studies of Coastal Oceans (PISCO) in order to produce a working, real-time mooring that is safely designed and fully functional.

2 Introduction

Low-oxygen areas of the ocean called “hypoxic zones” or “dead zones” can be found just off the Oregon and Washington coast. These dead zones have occurred every summer since 2002, killing bottom-dwelling sea-life. Scientists believe dead zones result from a combination of unusual circulation patterns that bring oxygen-poor water nearer to shore than usual and from increased phytoplankton blooms. The Partnership for Interdisciplinary Studies of Coastal Oceans (PISCO) is helping to unravel the cause of these events by monitoring levels of dissolved oxygen off the Oregon Coast.

Traditional oceanographic moorings store data in the instrument’s hard drive until they are retrieved. Servicing of traditional moorings requires the moorings to be recovered by boat, the data to be downloaded, and the moorings to be redeployed. A real-time mooring has the ability to transmit data directly from the mooring instruments to the researcher’s desk via a cell phone modem without any servicing. The PISCO group at Oregon State University (OSU) envisions an array of real-time moorings along the entire Oregon Coast that can continuously monitor levels of dissolved oxygen with little or no service. PISCO had taken the initial steps of procuring the necessary materials for a real-time mooring; however before the project was begun the mooring had not yet gone through a formal design nor construction process. This project is an interdisciplinary partnership between the Coastal and Ocean Engineering Program with the Department of Zoology at OSU in order to produce a working real-time mooring that is safely designed and fully functional.

2.1 Background

Off the Oregon Coast, dead zones appear to be correlated with of changes in atmospheric conditions. These conditions create an ocean river of nutrient-rich waters known as the California Current. In turn the California Current fuels the United States West Coast fisheries. Their productivity comes from wind driven upwelling of nutrient-rich waters from the deep. When these waters reach the surface and hit sunlight, tiny ocean plants known as “phytoplankton” bloom, creating food for small fish and shellfish that in turn feed larger marine animals up the food chain.

What’s happening off the Oregon coast, scientists believe, is that as land heats up, winds grow stronger and more persistent. Because the winds do not go slack as they used to, the upwelling is prolonged, producing a surplus of phytoplankton. There are not enough fish to consume all the phytoplankton, and it ultimately dies, and drifts down to the seafloor to decompose. Bacteria then take over, and in the process of breaking down the plant matter, they suck the oxygen out of the seawater making it unable to support most forms of sea life.

2.2 Objective

Measurements of hypoxic conditions along the Oregon coast are still rare. PISCO is looking at comparative patterns in ecosystem structure and processes and is particularly interested in summertime dead zones. Daily measurements of dissolved oxygen are needed to try and explain the hypoxia, and the speed at which the data can be retrieved and analyzed is also important. For this reason, a real-time mooring is desired at Strawberry Hill during the summer months.

2.2.1 Previous Work

PISCO utilizes an array of traditional oceanographic moorings off the Oregon coast as shown in Figure 1. The research findings to date have found that the Pacific Ocean off Oregon is characterized by intermittent, weak summer upwelling with periods of relaxation. PISCO also performs several cruises each year during the summer months that monitor physical and biological conditions in the water. This research follows up on PISCO studies that helped to uncover dead zones that killed bottom-dwelling sea-life along the central coast of Oregon in 2002.

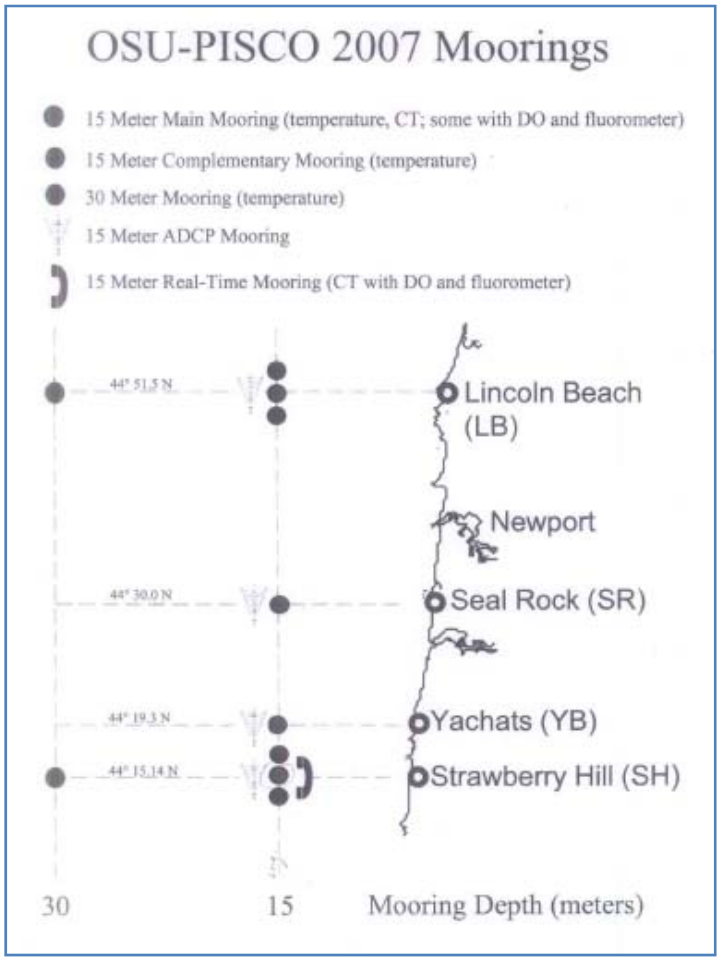

Figure 1: 2007 PISCO mooring locations

PISCO deploys and services all their moorings shown in Figure 1 by boat. They use the R/V Elakha, a 54-foot vessel, which is specially designed for oceanographic research. These moorings need service once a month in order to download data and change instrument batteries which means researchers must wait up to four weeks for dissolved oxygen data sets.

2.2.2 Benefits

The benefit of a real-time mooring is that it has the ability to transmit data to an internet protocol (IP) address via a cell phone modem. The transmission can be a scheduled or manually requested so that the most recent data is available to researchers. The real-time mooring only requires one deployment

and one recovery at the beginning and end of the summer. This saves funding, time, and effort since monthly R/V Elakha services are not needed. Finally, working on the ocean can be a rewarding but dangerous job. A real-time mooring at Strawberry Hill allows PISCO to accomplish its mission while keeping its researchers as safe as possible.

3 Site Conditions

This section contains information on the location of the real-time mooring and the expected site conditions including wave height, wave period, tidal amplitude, current, wind, and wave breaking.

3.1 Location

The site of the real-time mooring is called Strawberry Hill and is located at (44° 15' 6.95"N, 124° 7' 40.62"W) off the Oregon Coast. This location is 0.2 nautical miles or 0.37 km offshore and slightly south of Yachats as see in Figure 2. The local water depth at this location is 15 m.

Figure 2: Close-up view of real-time mooring location (Google Earth)

3.2 Environmental Data

Station 46050 at Stonewall Banks was selected as a source of environmental data since it is the closest NDBC buoy to Strawberry Hill. The relative proximity of these two locations is shown in Figure 3.

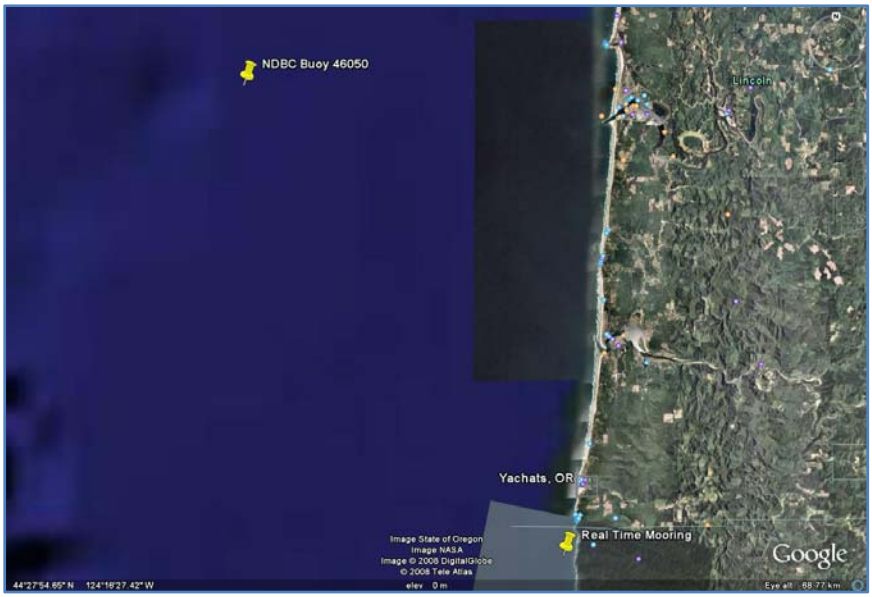

Figure 3: Real-time mooring and NDBC buoy locations (Google Earth)

A 10-year record of environmental data was collected from the National Data Buoy Center (NDBC) buoy 46050 (National Data Buoy Center, 2008). The NDBC buoy is shown in Figure 4 and is located 20 nautical miles or 37.04 km west of Newport, OR, at Stonewall Banks (44° 38’ 28”N, 124° 29’ 59”W). Other station information is as follows:

- Owned and maintained by National Data Buoy Center
- The local water depth at this location is 123 m
- 3-meter discus buoy
- Anemometer height: 5 m above site elevation
- Watch circle radius: 281 yards

Figure 4: NDBC Station 46050 – Stonewall Banks buoy

3.3 Wave Height

The real-time mooring will only be deployed during the summer months of May through September. The data from NDBC buoy 46050 (see Figure 5) shows that these months experience a smaller significant wave height as do months in the winter.

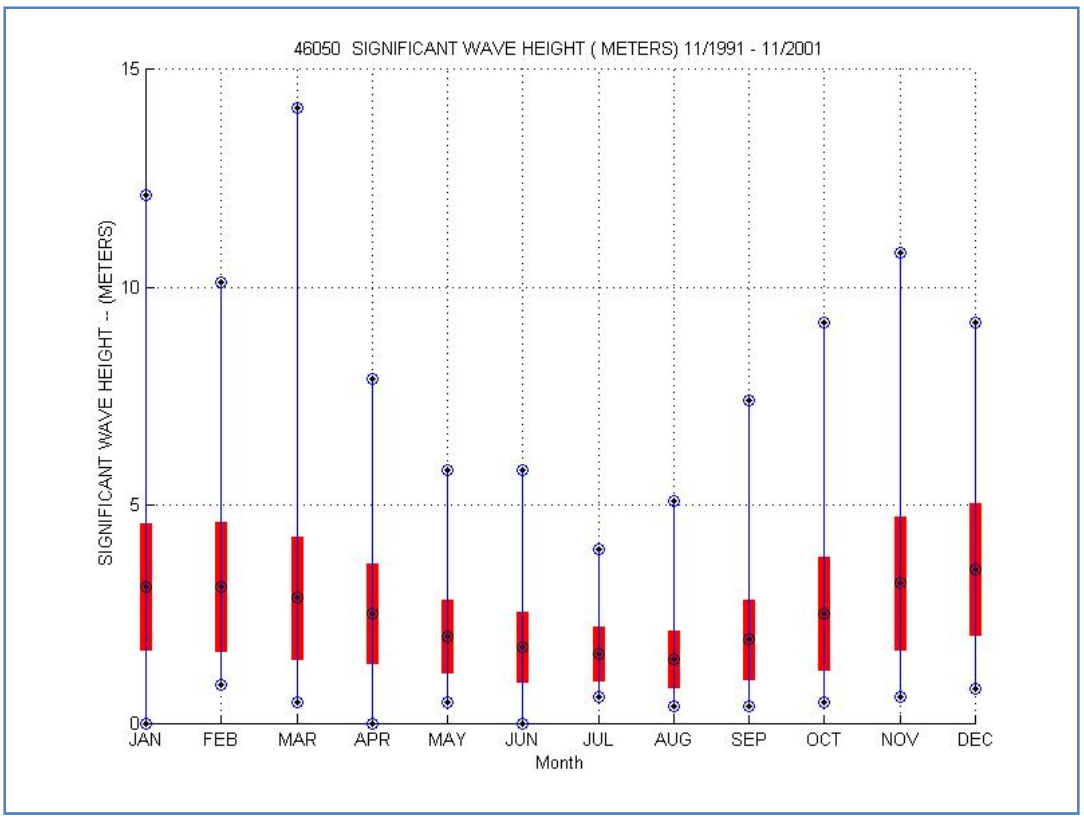

Figure 5: Significant wave height at NDBC station 46050

A design wave height was determined from the 10-year environmental data record (National Data Buoy Center, 2008) by performing a statistical analysis of extreme waves using the "peaks-over-threshold" method (Goda, 2000). This method is not an "annual maxima" or "total sample" method; instead it takes the peak heights of storm waves over a certain threshold value and compares them to a statistical distribution. The four distributions used for comparison are:

1. Fisher-Tippett type I (FT-I) or Gumbel distribution
2. Fisher-Tippett type II (FT-II) or Frechet distribution (k=10)
3. Weibull distribution (k=1.4)
4. Weibull distribution (k=2.0)

Where k is a non-dimensional shape parameter. The "peaks-over-threshold" method provides sample independency and homogeneity, and it can handle a large data set while still producing a small confidence interval.

A 5-year wave height was estimated for only the summer months of May through September. The number of records used, N, was 82 which corresponds to a wave height threshold of 5.0 m. Table 1 shows the calculations of the reduced variate, y(m), and the storm wave height, x(m) that are plotted in Figure 6.

Table 1: Results of "peaks-over-threshold" method for wave height

N, N_T	82
K=	10
λ=	8.20
ν=	1

	Ahat	**Bhat**	k	α	β
FT-I	0.441	5.101	-	0.440	0.120
FT-II	0.383	5.098	10.0	0.492	0.109
Weilbull	0.844	4.592	1.4	0.428	0.394
Weilbull	1.189	4.299	2.0	0.391	0.363

m	x_m	FT-I		FT-II (k=10)		Weilbull (k=1.4)		Weilbull (k=2.0)	
		F_m	y_m	F_m	y_m	F_m	y_m	F_m	y_m
1	7.5	0.9932	4.985	0.9938	6.623	0.9931	3.144	0.9926	2.215
2	7.0	0.9810	3.954	0.9816	4.900	0.9809	2.672	0.9805	1.984
3	7.0	0.9688	3.452	0.9695	4.153	0.9688	2.430	0.9683	1.858
4	6.5	0.9566	3.116	0.9573	3.677	0.9566	2.264	0.9562	1.769
5	6.5	0.9445	2.862	0.9451	3.330	0.9445	2.135	0.9440	1.698
80	5.0	0.0312	-1.244	0.0317	-1.165	0.0343	0.091	0.0334	0.184
81	5.0	0.0190	-1.377	0.0195	-1.281	0.0221	0.066	0.0213	0.147
82	5.0	0.0068	-1.607	0.0073	-1.472	0.0100	0.037	0.0091	0.096
Correlation		r^2=	0.891	r^2=	0.914	r^2=	0.903	r^2=	0.846
5 Year Wave		y_5=	4.401	y_5=	4.479	y_5=	2.885	y_5=	2.099
		x_5=	7.042	x_5=	6.814	x_5=	7.027	x_5=	6.795

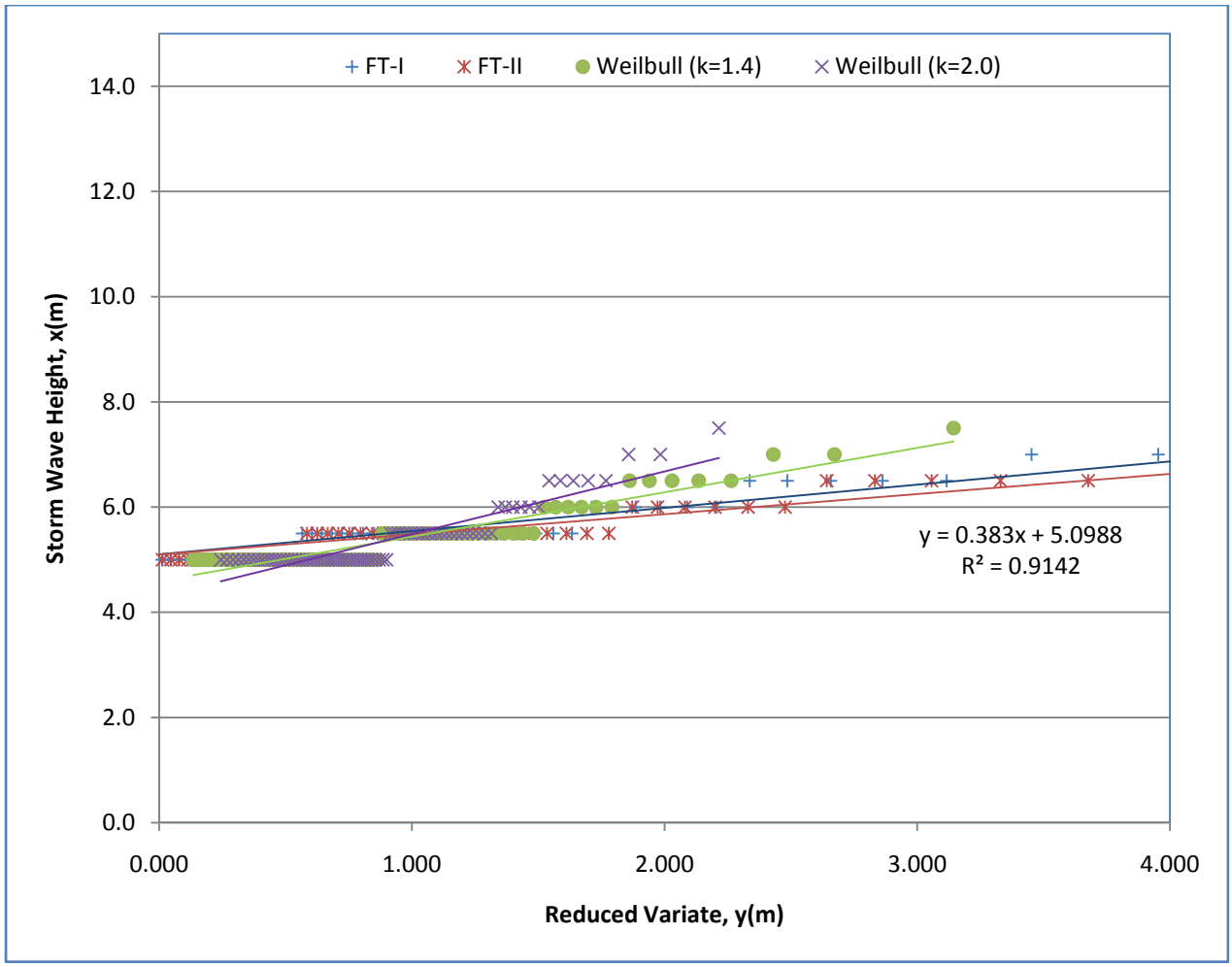

Figure 6: Fitting of data to four statistical distributions

The Fisher-Tippett type II (k=10) distribution yielded the best correlation with an r^2-value of 0.9142, and a 5-year wave height of 6.8 m was calculated. The 5-year wave height for summertime waves was the chosen design criterion because it best represents PISCO's planned use for the real-time mooring. Then entire wave height calculation is included in Appendix A.

3.4 Wave Period

The same analysis was applied to determine the wave period design condition. Figure 7 shows that these months experience a smaller average wave period than months in the winter.

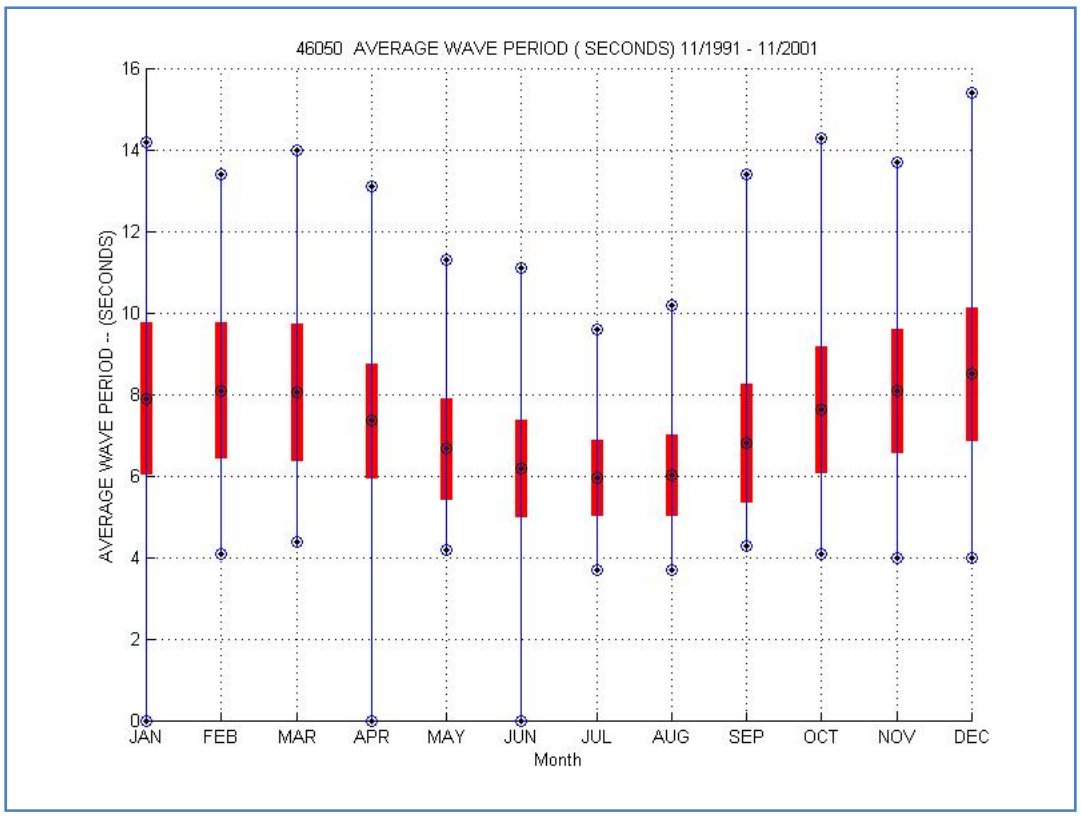

Figure 7: Average wave period at NDBC station 46050

The same NDBC buoy was used to determine the 5-year summertime wave period. The number of records used, N, was 110 which corresponds to a wave period threshold of 11.0 sec. The Weibull (k=1.4) distribution yielded the best correlation as seen in Appendix B, and a 5-year wave period of 13.3 s was calculated.

3.5 Tidal Amplitude

Tide data was used from the National Oceanic and Atmospheric Administration's (NOAA) Tides and Currents website (Tides and Currents, 2008). The closest tide gage to Strawberry Hill is located at South Beach, OR (44° 37' 30"N, 124° 2' 34.8"W) in Yaquina Bay. Figure 8, shows a plot of the daily highest and lowest water levels from May to September 2008.

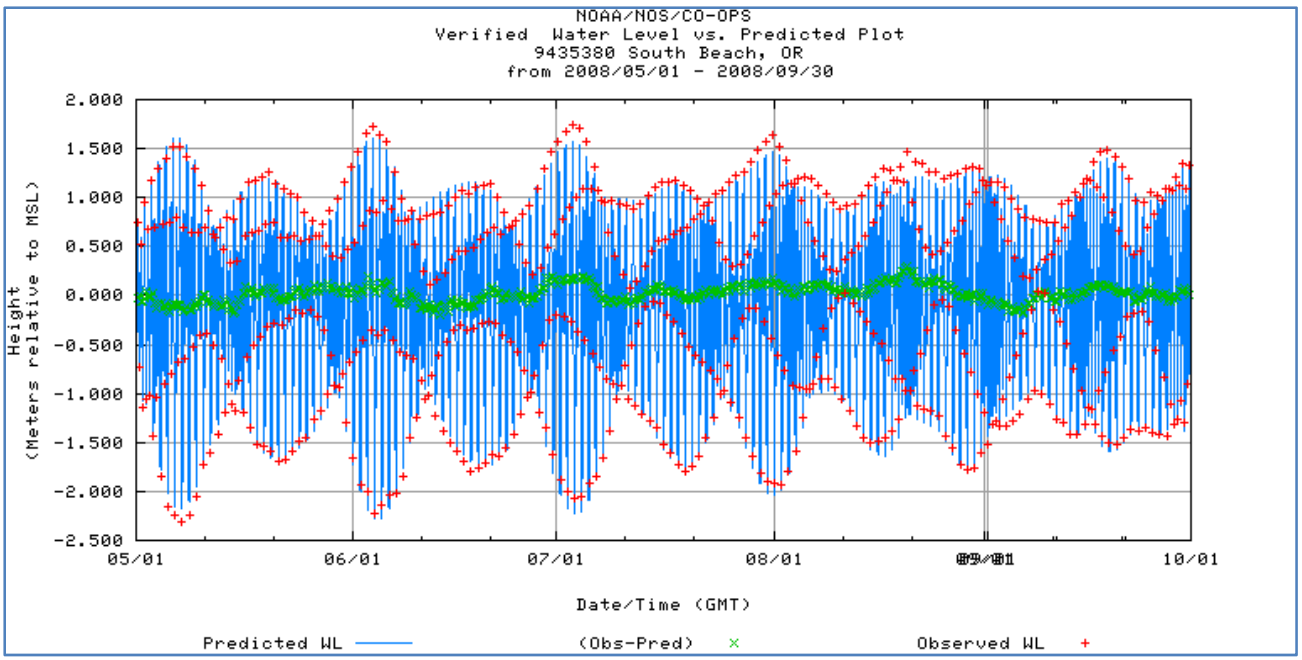

Figure 8: Tide levels at South Beach, OR

An average tide of 4 m is found inside the bay, but the real-time mooring is located offshore where fluctuations in water levels due to tides are less. Therefore a 2 m tide was used as the design condition for the real-time mooring at Strawberry Hill.

3.6 Current

Ocean currents have a great effect on the performance of a mooring due to drag forces. For this reason, site specific current data was needed for Strawberry Hill. PISCO provided an Acoustic Doppler Current Profiler (ADCP) record from 31 May 2006 to 8 September 2006 (S. Dudas, personal communication). This record was further analyzed in order to give a design surface current magnitude (top 10 m of water) and design bottom current magnitude (current at a single location, 1 m from the bottom). The data consists for measured daily averaged currents and the entire record is shown in Appendix C. Three design cases were considered when extracting a single set of values for summer time current:

1. **Mean surface current and mean bottom current**: Average value for the top 10 m of water and average value 1 m from the bottom for a three month record.
2. **Maximum surface current and its associated bottom current**: Maximum value for the top 10 m of water for a three month record and its corresponding (same day) value 1 m from the bottom.
3. **Maximum summation of surface current and bottom current**: Maximum summation value for the top 10 m of water and the value 1 m from the bottom for a single day during the three month record.

For this record, case 2 and 3 produced the same single set of values for summer time current. Case 1 gave a mean top current of 0.17 m/s and a mean bottom current of 0.07 m/s. Case 2 gave a maximum surface current of 0.37 m/s and a maximum bottom current of 0.19 m/s.

3.7 Wind

A design wind speed was established from the 10-year environmental data record (National Data Buoy Center, 2008) by performing a statistical analysis of extreme wind speeds using Goda's "peaks-over-threshold" method (Goda, 2000). A 5-year wind speed was estimated for only the summer months of May through September using the hourly average wind speed. The number of records used, N, was 84 which corresponds to a wind speed threshold of 26 knots. The Weibull (k=1.4) distribution yielded the best correlation as seen in Appendix D, and a 5-year wind speed of 33.7 knots (36.4 mph) or 16.3 m/s was calculated.

3.8 Wave Breaking

Wave breaking was calculated using the 5-year wave height of 6.8 m from Section 3.3 Wave Height and the 5-year wave period of 13.3 s from Section 3.4 Wave Period for both the NDBC buoy at Stonewall Banks and the real-time mooring at Strawberry Hill. To determine if a location is in deep, transitional, or shallow water, the following non-dimensional parameter for water depth was used: d/gT^2. To determine if waves are breaking at this location, the following non-dimensional parameter for wave height was used: H/gT^2. In each case, g is the acceleration due to gravity, T is wave period, d is water depth, and H is wave height.

3.8.1 Stonewall Banks

The non-dimensional parameter for water depth is:

$$\frac{d}{gT^2} = \frac{123}{9.81(13.3)^2} = 0.0709$$

And, the non-dimensional parameter for wave height is:

$$\frac{H}{gT^2} = \frac{6.8}{9.81(13.3)^2} = 0.0039$$

This point is plotted on Figure 9 in blue showing that the NDBC buoy at Stonewall Banks is in transitional water and the waves are not breaking.

3.8.2 Strawberry Hill

The non-dimensional parameter for water depth is:

$$\frac{d}{gT^2} = \frac{15}{9.81(13.3)^2} = 0.0086$$

And, the non-dimensional parameter for wave height is:

$$\frac{H}{gT^2} = \frac{6.8}{9.81(13.3)^2} = 0.0039$$

This point is plotted on Figure 9 in red showing that the real-time mooring at Strawberry Hill is in transitional water and the waves are still not breaking.

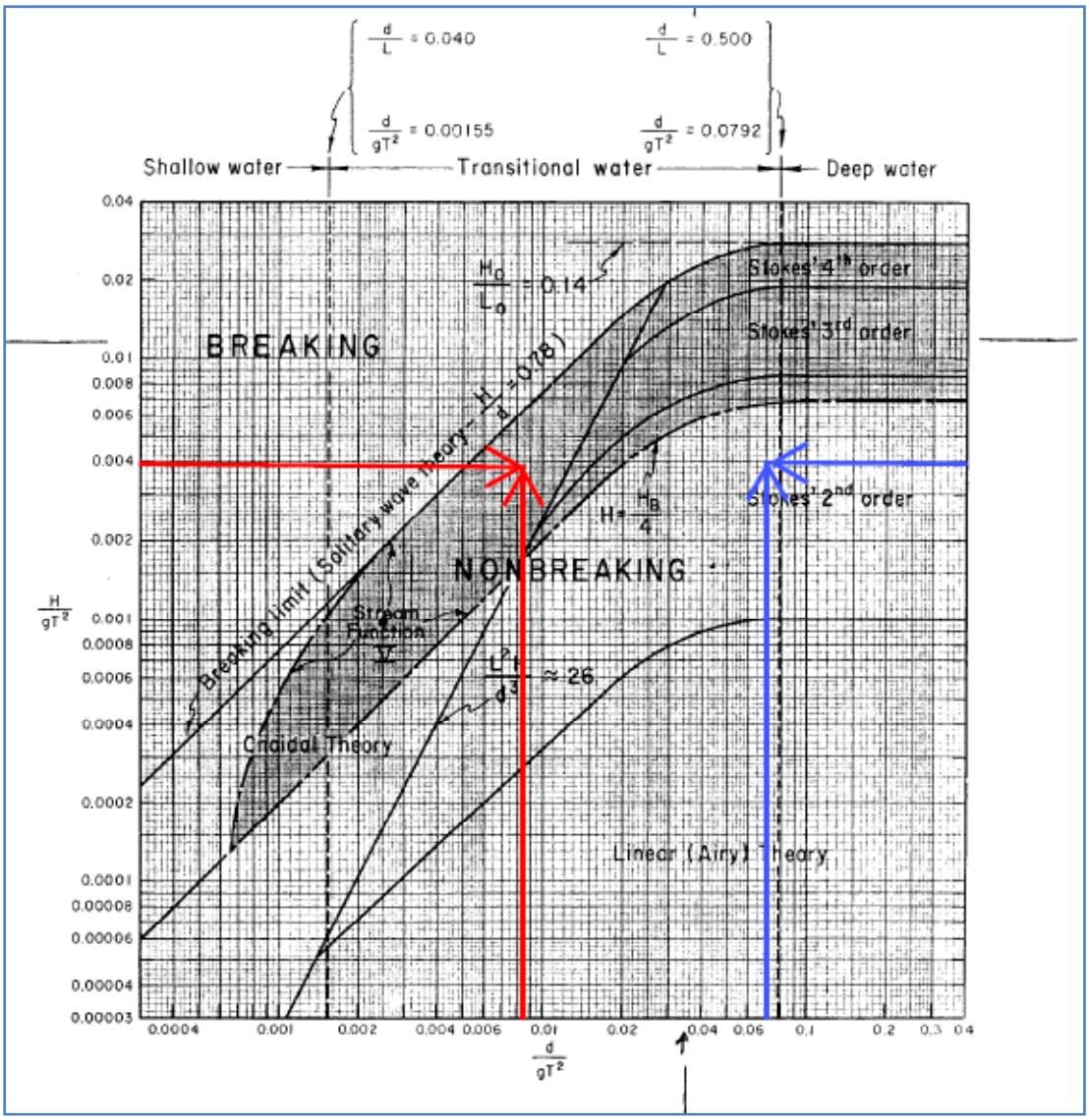

Figure 9: Regions of validity for various wave theories

Since Stonewall Banks and Strawberry Hill are both in transitional water without breaking waves, the significant wave height from Section 3.3 Wave Height of 6.8 m is considered the design wave height. Storm surge was not considered in the design or the analysis of the real-time mooring.

4 Design

This section describes the basic theory for this analysis and the iterative solution used to evaluate the mooring. It includes an initial sketch of the mooring and a design for the lengths of the mooring lines. It also includes a description of the individual elements of the real-time mooring, and both its static and

dynamic response to expected site conditions at Strawberry Hill. Finally, the results from these responses are tabulated in this section.

Mooring Design and Dynamics (MDD) is a software package written for Matlab® and used for designing and analyzing oceanographic moorings and towed bodies. It was developed by Richard K. Dewey at the Centre for Earth and Ocean Reach at The University of Victoria, British Columbia, Canada. MDD is a set of Matlab® routines that can be used to assist in the design and configuration of single point or single anchor moorings and the evaluation of mooring tension and shape under the influence of current and wind. MDD will predict the tension and angle at each mooring component, including the anchor, for which the safe mass will be evaluated in terms of the vertical and horizontal tensions. The package includes a database of standard mooring components which can be selected from pull down menus, and the database can be edited, expanded, and customized to include user specific elements(Dewey, 2007).

4.1 Basic Theory

This section defines forces acting on the real-time mooring due to buoyancy, drag, lift, tension. It also includes definitions of safe wet anchor mass, free fall speed, and elongation.

4.1.1 Buoyancy

The buoyancy of the elements in the real-time mooring is given in kilograms, where positive buoyancy represents objects that have an upward buoyancy force when submerged under water, and negative buoyancy represents a downward force. The negative buoyancy is also called weight, W, and it acts vertically downward through the element's center of gravity. The buoyancy of an element is equal to the weight of the displaced seawater and the buoyant force, F_B, is vertically upward through the center of buoyancy. If the element floats, then the mass of seawater displaced by the volume of the object is more than the mass of the object, and the buoyancy will be positive. If the element sinks, then the mass of seawater displaced is less than the mass of the device and the buoyancy will be negative. The center of buoyancy is also the centroid of the element's submerged volume. Finally, the elements immersed weight, W_I is defined in Equation 1.

$$W_I = F_B - W$$

Equation 1: Immersed weight

If W_I is positive, the element is positively buoyant (polypropylene subsurface floats), and if it is negative, the element is negatively buoyant (wire rope and shackles) (Randall, 1997). Steel retains approximately 87% of its weight in seawater so a factor of 0.87 must be multiplied to the immersed weight to get the equivalent dry steel mass. Concrete retains approximately 65% of its weight in seawater so a factor of 0.65 must also be multiplied to the immersed weight to get the equivalent dry concrete mass (Dewey, 2007).

4.1.2 Drag and Lift

Since the elements of the real-time mooring are either floating or submerged, it is also exposed to the flow of water (ocean currents), which results in drag and lift forces acting on the mooring elements. The drag force, F_D, consists of friction and pressure forces as a result of tangential and normal stresses acting on the surface of the elements. If the flow past the elements is laminar, then the shear (tangential), or friction, stresses dominate. When the flow is turbulent and the shape of the element is blunt the normal stresses (pressure) dominate. The resultant force is obtained by integrating the shear and pressure stresses over the area of the element and is called the resistance force. This force has two components called drag in the direction of flow and lift in the direction normal to the flow(Randall, 1997). Equation 2 is used to determine drag force, F_D. MDD does not calculate lift for the elements in the mooring.

$$F_D = \frac{1}{2}\rho C_D A_N U^2$$

Equation 2: Drag law

Where ρ is the fluid density, C_D is the coefficient of drag, A_N is the area projected on a plane normal to the fluid flow, A_L, and U is the average fluid velocity. The drag force is assumed to act through the centroid of the projected area, A_N (Randall, 1997).

MDD treat all elements as either cylinders or spheres. With the appropriate selection of a drag coefficient, this approximation provides sufficient accuracy for most oceanographic instruments. Spheres characterize devices whose surface area is "isotropic" or equal at any orientation, while cylinders are "anisotropic" and projected area and the resulting drag forces vary with respect to vertical and horizontal orientation (Dewey, 2007).

Drag coefficients are a function of Reynolds number, Re, as defined in Equation 3.

$$\mathrm{Re} = \frac{UD}{\nu}$$

Equation 3: Reynolds number

Where U is the velocity of the flow, D is the characteristic buoy dimension, and ν is the fluid kinematic viscosity. MDD assumes that Reynolds number of the flow past the object is relatively large, and verging on either the transition from laminar to turbulent flow (Re>100), or turbulent flow (Re >= 1000). Streamlined objects can have relatively low drag coefficients (0.1), while blunt objects that introduce considerable wake may have a drag coefficient as high as 3 to 4(Dewey, 2007).

MDD allows an element to be assigned a drag coefficient between 0 and 9.99. A typical drag coefficient for a 100 cm diameter, painted sphere is 0.65, while a 20 cm diameter sphere may have a drag coefficient as high as 1.0. In MDD, cylinders have a drag coefficient between 1.0 to 1.3, with larger cylinders having a slightly lower drag than small cylinders (Dewey, 2007).

4.1.3 Tension

The free body diagram for a submerged element moored in a current is shown in Figure 10. For static equilibrium to exist, the sum of the forces and moments must be equal to zero (Randall, 1997).

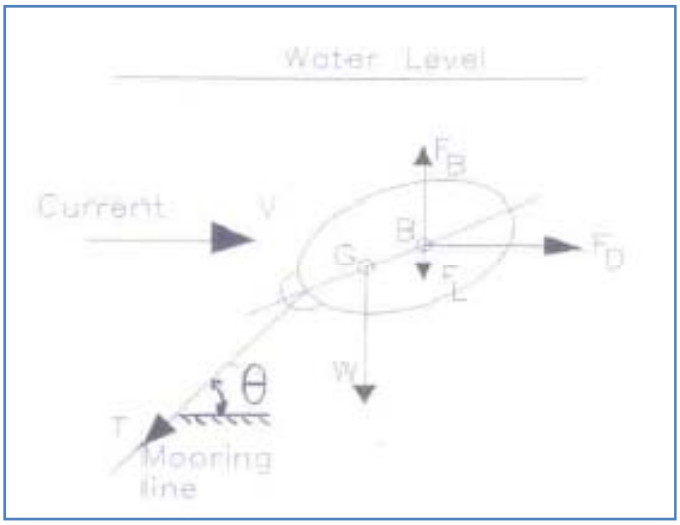

Figure 10: Free body diagram of a submerged element in current (Randall, 1997)

By summing the forces at the attachment point, the results are given in Equation 4 and Equation 5.

$$T_H = F_D$$

Equation 4: Horizontal component of tension

$$T_V = F_B - W$$

Equation 5: Vertical component of tension

Where T_H and T_V are the horizontal and vertical tensions in the submerged element; the forces, F_D and F_B are the drag and buoyant forces respectively, and W is the weight of the buoy. The resultant tension is defined in Equation 6:

$$T = \sqrt{T_H^2 + T_V^2}$$

Equation 6: Resultant tension

And the angle between the element and the horizontal is found by Equation 7.

$$\theta = \tan^{-1}\frac{T_V}{T_H}$$

Equation 7: Resultant angle

4.1.4 Safe Wet Anchor Mass

The safe wet anchor mass is the force required to hold the real-time mooring in position based on both the vertical and horizontal tensions. MDD calculates this force from the equal and opposite tension that the fully submerged, mooring under current exerts on the anchor. The tension acting on the anchor can be inverted into an estimate of the required anchor weight. MDD assumes that the anchor is stationary with respect to the ground, regardless of its mass. Factors of safety for both horizontal and vertical loads are used to estimate a realistic, safe wet anchor mass according to Equation 8 which incorporates drag and lift safety factors, and is adopted from the Mooring Group at the Woods Hole Oceanographic Institution(Dewey, 2007).

$$SafeWetAnchorMass = 1.5\left(W_{anchor-vertical} + \frac{W_{anchor-horizontal}}{0.6} \right)$$

Equation 8: Safe wet anchor mass

MDD also gives the equivalent safe dry anchor mass for steel and concrete. MDD has the capability of estimating the tension and fall speed during a free fall descent, but this capability was not used. MDD also has the capability of estimating elongation in the mooring line under tension, but this capability was not used either.

4.2 Iterative Solution

For each element in the real-time mooring, there are three equations and six unknowns:

- Tension from above (in the x, y, and z-directions)
- Tension from below (in the x, y, and z-directions)

The direction from which these tensions act are based on the two spherical coordinate angles each mooring element makes from the vertical z-axis, ψ, and the x-y plane, θ.

To start, the spar buoy has no tension from above and therefore, three equations and three unknowns remain. Since the tension and associated tension angles between any two elements are equal and opposite, the method of solution is to estimate the lower tension and angles for the upper element, in this case the buoy, and then subsequently estimate the tension and angles below each subsequent element. The resulting set of angles, ψ and θ, and element lengths determines the exact x-y-z-position of each mooring element relative to the anchor. Also, once the top of the anchor is reached, the resulting tension is a direct estimate of the necessary force needed to secure the mooring. MDD assumes that the anchor is stationary with respect to the ground, regardless of its mass (Dewey, 2007).

Specifically, the mooring solution is obtained as follows:

1. The flow velocity and water density profiles and the mooring sections are interpolated to approximately one meter vertical resolution using linear interpolation.

2. The force due to drag, F_D, from Equation 2 is now Q. The drag, Q, in each direction (x, y, and z) acting on each mooring element is calculated by Equation 9.

$$F_D = Q_i = \frac{1}{2}\rho_w C_{Di} A_i U U_i$$

Equation 9: Force due to drag

Where Q_i is the drag on element "i" in the direction "i" (x, y, or z), ρ_w is the density of seawater at the depth of the mooring element, U_i is the velocity component in the i-direction, C_{Di} is a drag coefficient appropriate for the shape of the element, A_i is the projected area in the i-direction, U_i is the velocity in the i-direction, and U is the velocity magnitude from Equation 10.

$$U = \sqrt{U^2 + V^2 + W^2}$$

Equation 10: Total vector magnitude of velocity

3. Once the drag force, Q_i, on each element or each interpolated segment of the mooring has been calculated, then the tension, T_i, and the two spherical coordinate angles each mooring element makes from the vertical z-axis, ψ, and the x-y plane, θ, necessary to hold that element in place (in the current) can be estimated. This is calculated by solving Equation 11 in the x, y, and z-directions.

$$\begin{aligned} Q_{xi} + T_i \cos\theta_i \sin\psi_i &= T_{i+1} \cos\theta_{i+1} \sin\psi_{i+1} \\ Q_{yi} + T_i \sin\theta_i \sin\psi_i &= T_{i+1} \sin\theta_{i+1} \sin\psi_{i+1} \\ B_i g + Q_{zi} + T_i \cos\psi_i &= T_{i+1} \cos\psi_{i+1} \end{aligned}$$

Equation 11: Component equations of tension

Where B_i is the buoyancy of the element, g is the acceleration due to gravity, and Q_{xi}, Q_{yi} and Q_{zi} are the respective drag forces. The tension below this element is T_{i+1}, with spherical coordinate angles ψ_{i+1} and θ_{i+1}.

4. Figure 11 shows the angles and hinge-like characteristics for an element E_i suspended in the middle of the mooring. Every mooring component and every interpolated segment of the mooring is considered an element. In this way, the mooring is flexible and can adjust to any necessary shape according to the velocity profile and associated drag on each mooring element.

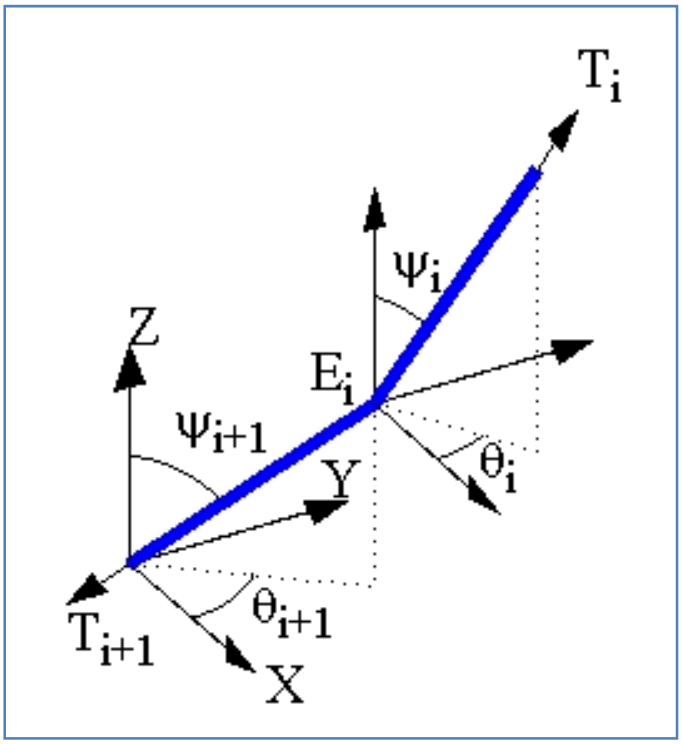

Figure 11: Orientation of the tension vectors (Dewey, 2007)

5. Once all of the tensions and angles have been calculated, the position of each element can be calculated by Equation 12.

$$X_i = X_{i+1} + L_i \cos\theta_i \sin\psi_i$$
$$Y_i = Y_{i+1} + L_i \sin\theta_i \sin\psi_i$$
$$Z_i = Z_{i+1} + L_i \cos\psi_i$$

Equation 12: Component equations of position

Where X, Y, and Z are the position of the element relative to the anchor and L_i is the length of each element.

MDD will display the position, the tensions, and the appropriate angles at the top and bottom of each element of the mooring (Dewey, 2007).

Mooring Sketch

The real-time mooring began with an initial design and drawing as seen in Figure 12.

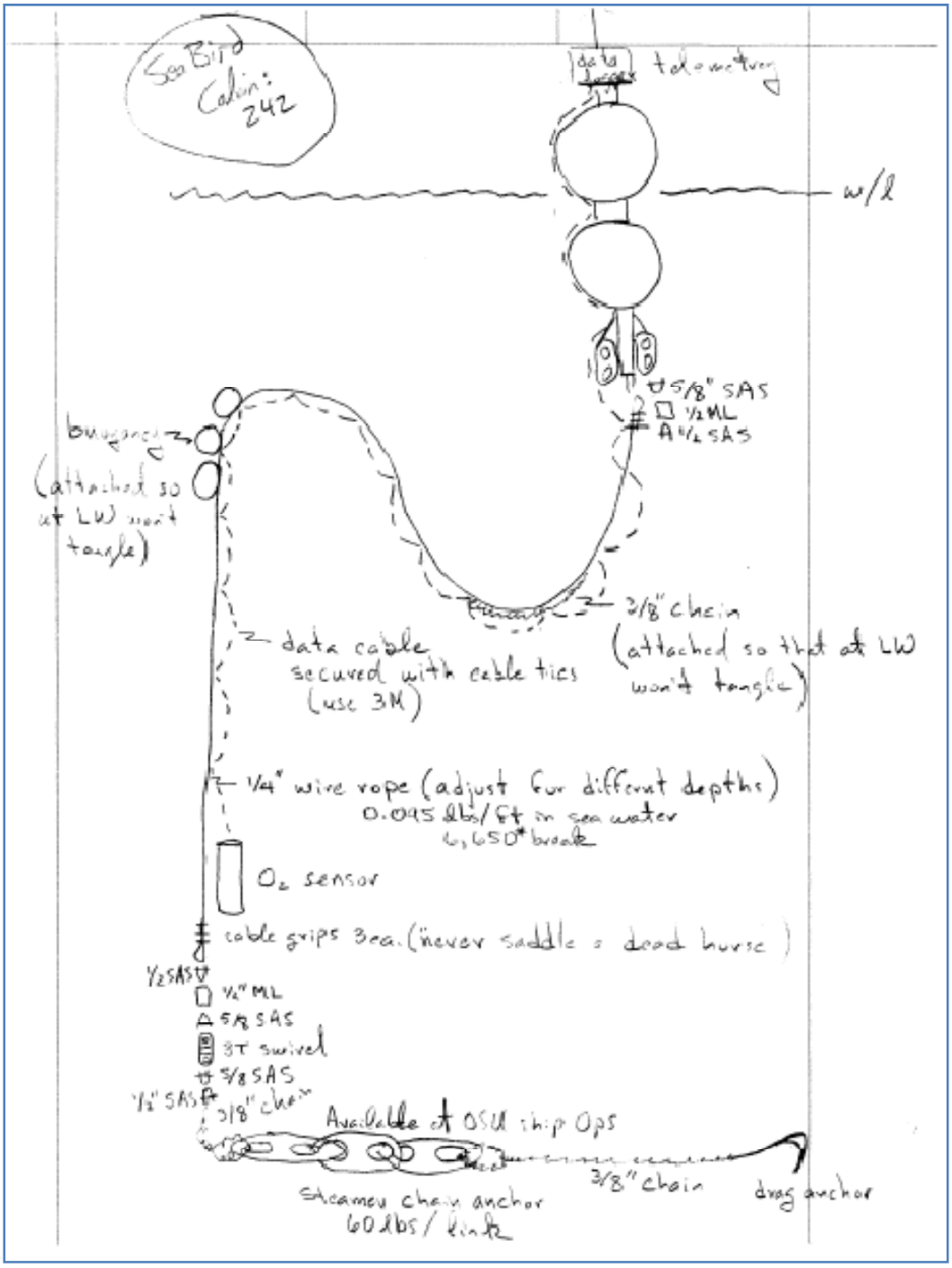

Figure 12: Original sketch of real-time mooring

4.3 Mooring Lengths

The mooring design shown in Figure 12 is a combination of a lower taut section, held up by the subsurface floats, and an upper top line that connects to the spar buoy. The instrument was mounted 2 m from the bottom and is kept in position by a series of subsurface floats. The data cable must run from the instrument, past the subsurface floats, along the rest of the mooring line, to the buoy, and into the datalogger. Since the length of data cable available from PISCO was a limiting factor, a rather direct route is needed from the instrument to the datalogger. In order to keep the mooring and data cable from tangling, an S-shaped mooring design was employed by connecting a length of negatively buoyant chain between the subsurface floats and the buoy. The weight of this chain actually pulls the buoy and subsurface floats apart. There is a slight chance that the buoy could drift directly over the subsurface floats where the mooring line and chain could touch, but the smooth connections throughout the mooring should keep it from tangling.

The design dimensions of the mooring are limited by the depth of the subsurface floats and the amount of slack in the top line or the mooring line between the subsurface floats and the buoy. The mooring design is site specific and depends directly on the water depth (including tidal amplitude) and the expected wave heights. Two moorings were designed and constructed for this project. The first mooring was designed for Yaquina Bay in order to test the spar buoy's performance in a protected location. The second mooring was designed for an ocean deployment at Strawberry Hill.

4.3.1 Yaquina Bay

At mean sea level, the depth of water at the Ship Ops pier is 6 m. Since this location is inside Yaquina Bay, a 4-meter tidal amplitude from Section 3.5 Tidal Amplitude is considered, and it is assumed that there are no waves. The design for the test mooring at Yaquina Bay can be seen in Figure 13.

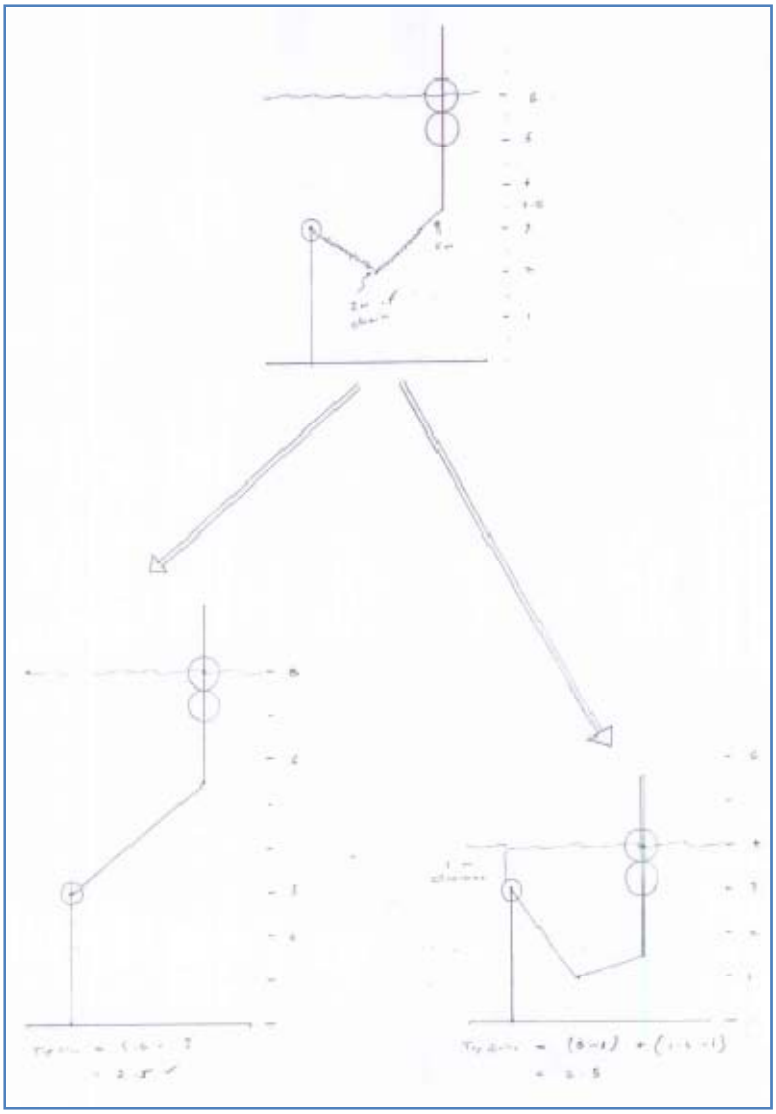

Figure 13: Mooring diagram for Yaquina Bay

At low tide (right side of Figure 13) the expected water depth is at 4 m. In order to give a 1 m clearance between the subsurface float and the surface of the water, the subsurface floats will be located 3 m from the bottom. This test mooring did not include an instrument so the bottom of the S-shaped top line was able to hang only 1 m from the bottom. Since the bottom of the buoy is at 1.5 m, the bottom of the top line is at 1 m, and the subsurface floats are at 3 m, the maximum length that the top line can be is 2.5 m. At high tide (left side of Figure 13) the expected water depth is at 8m, the bottom of the buoy is at 5.5 m, and the 2.5 m long top line just reaches to the subsurface floats at a depth of 3 m.

4.3.2 Strawberry Hill

At mean sea level, the depth of water at Strawberry Hill is 15 m. Since this mooring is located offshore where fluctuations in water levels due to tides are less, a 2-meter tidal amplitude from Section 3.5 Tidal Amplitude is considered. The 5-year wave height of 6.8 m was used and these waves are not breaking per Section 3.8. The design for the real-time mooring at Yaquina Bay can be seen in Figure 14.

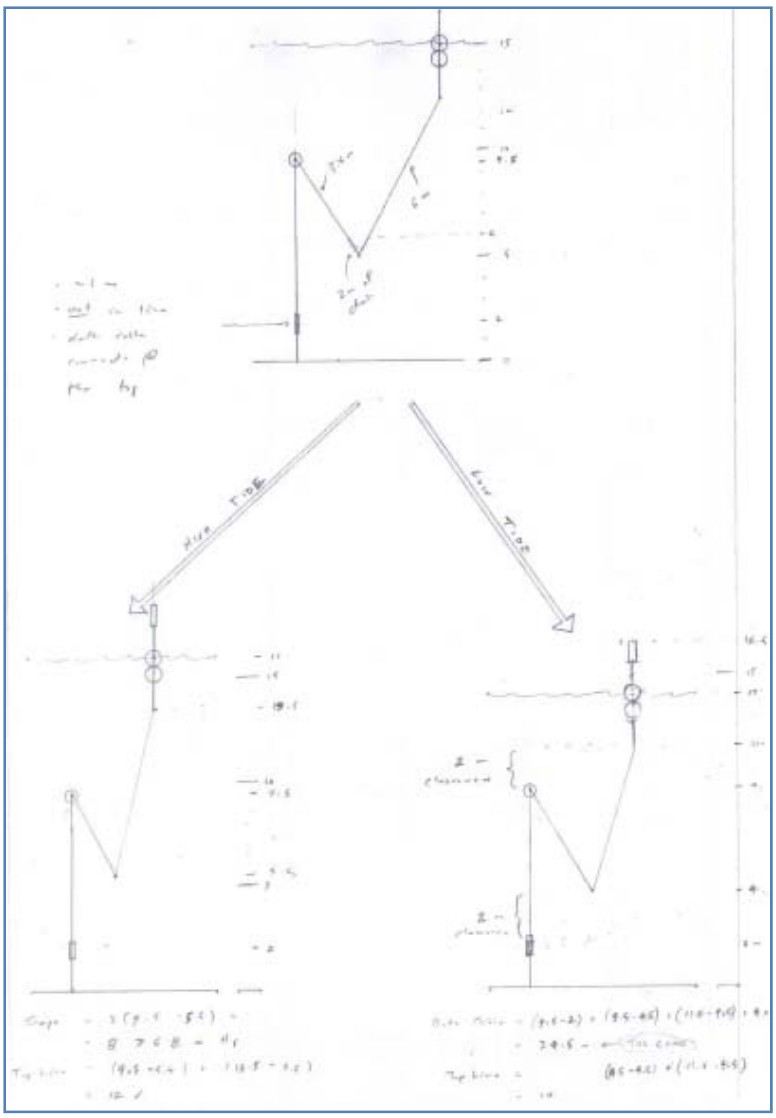

Figure 14: Mooring diagram for Strawberry Hill

At low tide (right side of Figure 14) the expected water depth is at 14 m. In order to give a 2 m clearance between the subsurface float and the bottom of the spar buoy, the subsurface floats will be located 9.5 m from the bottom. This keeps the bottom of the spar buoy from colliding with the subsurface floats. The approximately 1-m long instrument for the real-time mooring is centered 2 m from the bottom so that the top of the instrument is at 2.5 m. There is another 2 m clearance between the instrument and the bottom of the S-shaped top line which keeps the top line from snagging on the instrument. Since the bottom of the buoy is at 11.5 m, the bottom of the top line is at 4.5 m, and the subsurface floats are at 9.5 m, the maximum length of that the top line can be is 12 m. At high tide (left side of Figure 14) the expected water depth is at 16m, the bottom of the buoy is at 13.5 m, and the 12 m top line still has 8 m of slack which can easily compensate for a 5-year wave height of 6.8 m.

4.4 Mooring Elements

Figure 15 shows all the components used in the real-time mooring at Strawberry Hill. This drawing includes broken-out details of all mooring connections.

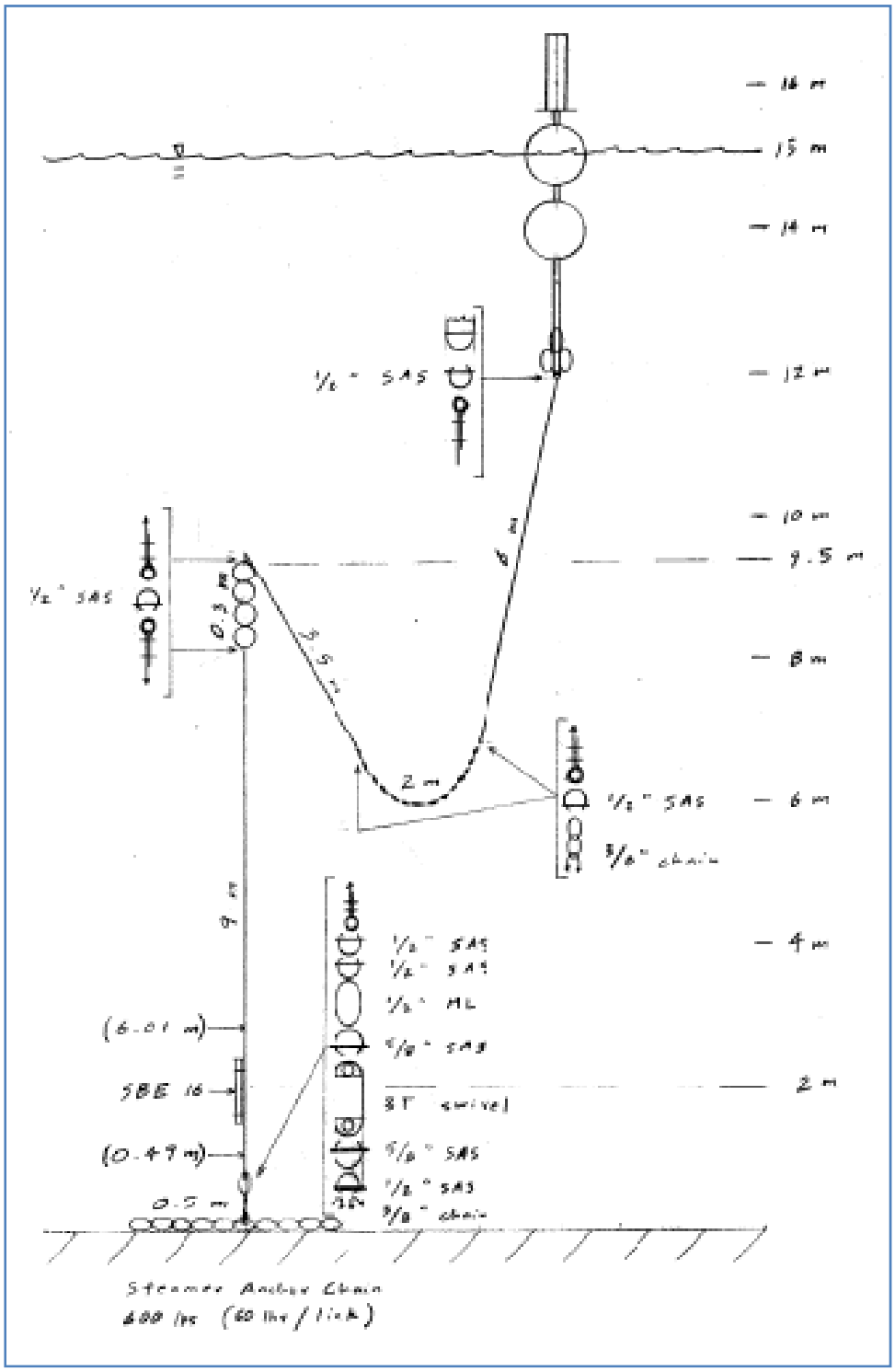

Figure 15: Real-time mooring drawing

Every individual component was loaded in to MDD and can be seen in Table 2 in its entirety from top to bottom including the 24.81 m total length of the real-time mooring.

Table 2: Component list

#	Mooring Element	Length *m*	#	Mooring Element	Length *m*
1	SparWithMount	3.66	13	1/2 shackle	0.08
2	1/2 shackle	0.08	14	1/4 wire/jack	6.01
3	1/4 wire/jack	6.00	15	SBE-16	0.45
4	1/2 shackle	0.08	16	1/4 wire/jack	0.49
5	3/8 chain SL	2.00	17	1/2 shackle	0.08
6	1/2 shackle	0.08	18	1/2 shackle	0.08
7	1/4 wire/jack	3.50	19	1/2 galv link	0.10
8	1/2 shackle	0.08	20	5/8 shackle	0.07
9	10"Castro	0.25	21	3T Crosby Swivel	0.18
10	10"Castro	0.25	22	5/8 shackle	0.07
11	10"Castro	0.25	23	1/2 shackle	0.08
12	10"Castro	0.25	24	3/8 chain SL	0.18
			25	600 lb chain	0.46
				Total Length =	**24.81 m**

In order to model the spar buoy as closely as possible, a custom flotation device was created in MDD. It was named “SparWithMount” and assigned a material type of steel. Under most conditions, the top of the buoy is above the surface and the remainder is below; however, this conservative design treats the buoy as subsurface when calculating the buoy’s buoyant force. The buoyancy was determined by taking the spar buoy’s 250 lbs of buoyancy and subtracting the weight of the data logger, 15 lbs, the battery, 32 lbs, and the equipment mount, 83 lbs. Since steel retains approximately 87% of its weight in seawater (Dewey, 2007), a factor of 0.87 was also multiplied.

$$(250lbs - 15lbs - 32lbs - 83lbs) \times 0.87 = 104.4lbs \approx 47.36kg$$

The buoyancy of the "SparWithMount" is 47.36 kg in the positive or upward direction. In MDD, elements may be modeled with either a single cylinders or spheres. MDD considers the element rigid and only allows movement between elements. Since the spar buoy has a long rigid shape, a cylindrical geometry was chosen for "SparWithMount", and it was assigned a length of 366 cm (equal to the actual length of 12 ft). However, the width of the buoy changes along its vertical length, so the average width or effective area was calculated in order to estimate the drag most accurately while continuing to model the buoy as a single rigid element. An effective width of 37.9 cm as calculated in Table 3 below.

Table 3: Effective width

	Length	Width	Area	
	ft	*ft*	ft^2	
Top with Mounting Plate	0.50	0.33	0.1665	
Upper Float	2.50	2.50	6.25	
Float Connection	0.50	0.50	0.25	
Lower Float	2.50	2.50	6.25	
Bottom tube and Counter Weight	6.00	0.33	2.00	
		Total Area =	14.91	ft^2
		Total Length =	12	ft
		Effective Width =	1.24	ft
		Effective Width =	**37.88**	**cm**

Finally, a drag coefficient of 1.1 was assigned since MDD recommends using drag coefficients between 1.0 and 1.3 for cylinders and the spar buoy is a smoothly painted object.

In order to model the steamer chain anchor used in the real-time mooring, a custom anchor was created. It was named "600 lb chain" and assigned a material type of steel. The weight was determined by multiplying a specified value or 60 lbs per link for this type of chain by the 10 links in the chain. Again, steel retains approximately 87% of its weight in seawater (Dewey, 2007), and a factor of 0.87 was also multiplied.

$$(60lbs/link \times 10links) \times 0.87 = 522.0lbs \approx 236.8kg$$

The weight of the "600 lb chain" is 236.8 kg in the negative or in the downward direction. A cylindrical geometry was chosen for "600 lb chain", and it was assigned a length of 45.7 cm (or a 1.5 ft high pile of chain) and width of 121.9 cm (or a 4 foot wide pile of chain.) A drag coefficient of 1.3 was assigned since MDD recommends using drag coefficients between 1.0 and 1.3 for cylinders and the anchor chain has a rough, corroded surface.

The remaining mooring components for the real-time mooring were available in the MDD database. The individual specifications for all elements of the mooring are shown in Table 4 below. Elements that have a given width are modeled as cylinders and elements with a given diameter are modeled as spheres.

Table 4: Component specifications

Mooring Element	Length	Width	Diameter	Buoyancy	Drag	Material Type	Load	
	cm	*cm*	*cm*	*kg*	Coefficient		*lbs*	*kg*
SparWithMount	366.0	37.9		47.36	1.1	Steel		unknown
10"Castro	25.0		25.0	4.30	0.65	Polypropylene		n/a
1/4 wire/jack	variable	0.8		-0.13	1.3	Steel	6750	3062
3/8 chain SL	variable	2.2		-2.33	1.3	Steel	2625	1191
3T Crosby Swivel	18.0	7.5		-4.17	1.3	Steel	6000	2722
5/8 shackle	6.5	5.0		-0.65	1.3	Steel	6500	2948
1/2 shackle	8.0	2.5		-0.30	1.3	Steel	4000	1814
1/2 galv link	10.0	2.5		-0.20	1.3	Steel	2900	1315
SBE-16	45.0	8.0		-10.00	1.3	Steel		n/a
600 lb chain	45.7	121.9		-236.80	1.3	Steel		unknown

The load ratings for the real-time mooring elements are also listed in Table 4. These values were referenced from Buoy Engineering (Berteaux, 1976) but were given a range of definitions: breaking load, working load, safe load, and safe working load. These loads are generally defined as some fraction of the ultimate breaking strength, for example,

Ultimate Breaking Strength x 90% = Breaking Load

Ultimate Breaking Strength = 4 x Working Load

Ultimate Breaking Strength = 6 x Safe Load

However, the factors of safety were not given and the values were taken directly from the reference.

4.5 Mooring Evaluation

This section describes how the environmental conditions at Strawberry Hill are loaded into MDD so that the response of the real-time mooring may be evaluated.

4.5.1 Load Environmental Conditions

MDD requires a velocity profile in order to evaluate the real-time mooring. This profile is a combination of current and wind velocities in opposing, perpendicular, and like directions.

4.5.1.1 Current

MDD was loaded with the two current profiles from Section 3.6 Current. The direction of the current is not important since a mooring responds the same way to current in any direction. This is also where the depth of water is specified in MDD.

4.5.1.2 Wind

MDD was also given a surface wind speed which applies an extra velocity kick to the upper ocean current speeds. Two percent of the wind speed is added to the surface current speed, and it decreases linearly to a depth that increases with wind speed. The 2% velocity kick penetrates to depths below the surface at approximately 1 m for every m/s of wind speed. The maximum wind penetration is 80% of the water column, assuming that a bottom boundary layer will exist within which wind forcing is negligible (Dewey, 2007). At Strawberry Hill, a 16.3 m/s (Section 3.6) wind penetrates an additional linearly decreasing velocity profile down about 12 m and 14.7 meters with waves.

4.5.1.3 Density

By default, MDD assumes a simple linearly stratified ocean with the density of seawater ranging from 1024 kg/m^3 at surface to 1026 kg/m^3 at bottom.

4.5.1.4 Waves

Waves acting on buoys also add a resistance force, but this force is usually small and neglected (Randall, 1997). MDD does not include any analysis of waves or wave forces although future versions may include waves and more truly dynamic forcing of moorings. For this analysis, waves were considered by evaluating the mooring at the instant it was at the crest of the 5-year wave calculated in Section 3.3. This was done by increasing the depth of water by half of the extreme wave height, H_5, or 3.4 m.

4.5.2 Evaluate Solution

The mathematical solution is evaluated using an iterative approach, repositioning the mooring components in the water column according to the element angle and position after each iteration. First, a solution is sought with a no flow condition. This provides an estimate of the component heights in the water column under tension, but without currents. Then, a solution is sought with the mooring forced by the specified velocity profile. Once the vertical position of the "SparWithMount" changes by less than 0.01 m between iterations, it is assumed a solution has been found (Dewey, 2007).

The "tilt" or angle of each element is taken into account when estimating the drag force and the projected area. The drag on spheres is not affected since spheres are isotropic. For cylindrical elements that are anisotropic, several factors change when the mooring element is tilted:

- The projected area changes.
- The drag is broken into tangential and normal components for each current direction acting on the element.

For example tilted wire rope, which is treated as cylinder segments, will have both a reduced projected area and drag coefficient to a horizontal current, but increased exposure and drag to a vertical current (Dewey, 2007).

A "surface solution" is found when the topmost element, in this case the spar buoy, remains on ocean surface. The mooring will not use all of the buoyancy of the top floatation device, leaving a portion of the floatation above water. This reduces both the "effective" or used buoyancy of the top floatation device, and the drag of the float, proportional to its portion in the water. For surface solutions in MDD, the approximate "percentage of the surface buoyancy" or the percentage of the top floatation device used to hold the mooring in position is given in the evaluation. Also shown are the total tension on the anchor and its vertical and horizontal components, the safe wet anchor mass, the safe dry steel and concrete anchor masses, and the weight under the anchor (Dewey, 2007). An example of an MDD evaluation is shown below and in Figure 16. These conditions represent Case 2 later on in Section 4.7.

Height[m]	*U [m/s]*	*V [m/s]*	*W [m/s]*	*Density [kg/m^3]*
15.00	*0.17*	*0.00*	*0.00*	*1024.00*
5.00	*0.17*	*0.00*	*0.00*	*1025.33*
1.00	*0.07*	*0.00*	*0.00*	*1025.87*
0.00	*0.00*	*0.00*	*0.00*	*1026.00*

First, find neutral (no current) mooring component positions.
.....
This is (starting off as) a potential surface float mooring
Searching for a converged solution.
.....
This is a surface solution, using 13% of the surface buoyancy.
Total Tension on Anchor [kg] = 1.9
Vertical load [kg] = -1.6 Horizontal load [kg] = 1.0
Safe wet anchor mass = -0.1 [kg] = -0.2 [lb]
Safe dry steel anchor mass = -0.1 [kg] = -0.2 [lb]
Safe dry concrete anchor mass = -0.1 [kg] = -0.3 [lb]
Weight under anchor = -235.1 [kg] (negative is down)

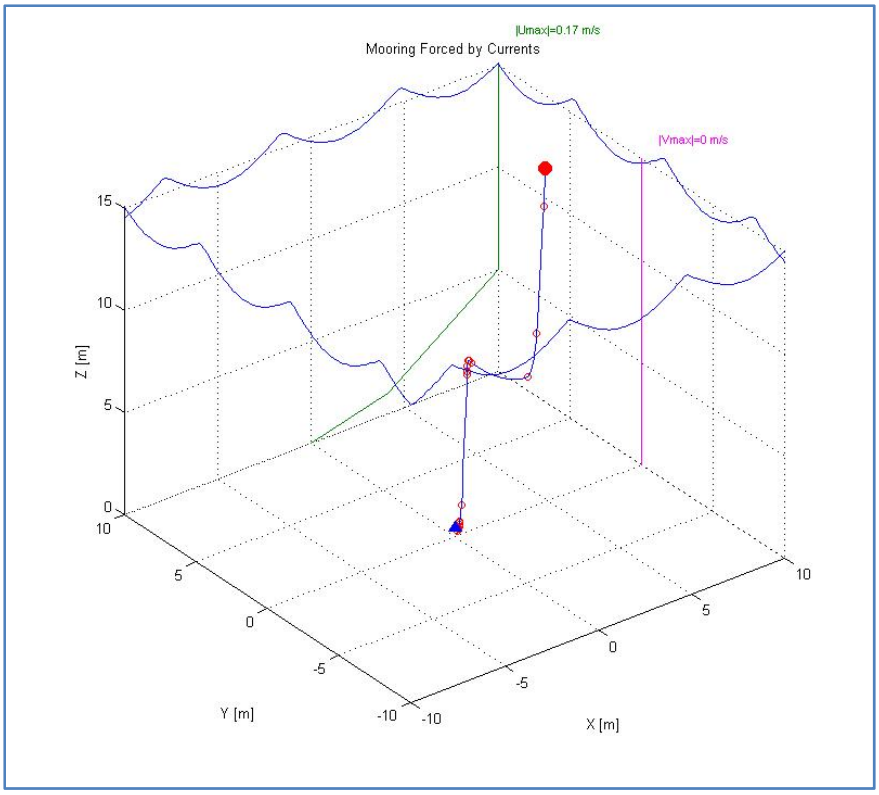

Figure 16: Mooring Plot in mean current

Once the mooring has been evaluated, then mooring elements can be listed by the component number and name, the physical length of the component, its buoyancy in kilograms, the height to the middle of the component when forced by the specified currents, the displacement in each direction (dZ, dX, and dY) from the vertical mooring in a no flow condition, the tension at the top and bottom of each element, and the angle in degrees from the vertical at the top and bottom of each element.

Table 5: Mooring evaluation in mean current

#	Mooring Element	Length	Buoyancy	Height	dZ	dX	dY	Tension		Angle	
								Top	Bottom	Top	Bottom
		m	kg	m	m	m	m	kg	kg	°	°
1	SparWithMount	3.66	47.36	16.39	0.1	5.2	0.0	0.0	5.9	2.8	2.8
2	1/2 shackle	0.08	-0.30	14.52	0.1	5.1	0.0	5.9	5.6	2.8	3.0
3	1/4 wire/jack	6.00	-0.13					5.6	4.8	3.0	4.5
4	1/2 shackle	0.08	-0.30	8.45	0.0	4.7	0.0	4.8	4.5	4.5	4.8
5	3/8 chain SL	2.00	-2.33					4.5	0.5	4.8	94.2
6	1/2 shackle	0.08	-0.30	6.58	0.2	4.1	0.0	0.5	0.7	94.2	111.2
7	1/4 wire/jack	3.50	-0.13					0.7	1.0	111.2	126.5
8	1/2 shackle	0.08	-0.30	8.31	0.1	1.0	0.0	1.0	1.3	126.5	133.6
9	10"Castro	0.25	4.30	8.42	0.1	0.9	0.0	1.3	3.1	133.6	9.4
10	10"Castro	0.25	4.30	8.38	0.1	0.8	0.0	3.1	7.4	9.4	4.3
11	10"Castro	0.25	4.30	8.13	0.1	0.7	0.0	7.4	11.7	4.3	3.0
12	10"Castro	0.25	4.30	7.88	0.1	0.7	0.0	11.7	16.0	3.0	2.4
13	1/2 shackle	0.08	-0.30	7.72	0.1	0.7	0.0	16.0	15.7	2.4	2.4
14	1/4 wire/jack	6.01	-0.13					15.7	14.9	2.4	2.8
15	SBE-16	0.45	-10.00	1.45	0.1	0.4	0.0	14.9	4.9	2.8	8.6
16	1/4 wire/jack	0.49	-0.13					4.9	4.9	8.6	8.7
17	1/2 shackle	0.08	-0.30	0.70	0.0	0.3	0.0	4.9	4.6	8.7	9.3
18	1/2 shackle	0.08	-0.30	0.62	0.0	0.3	0.0	4.6	4.3	9.3	10.0
19	1/2 galv link	0.10	-0.20	0.53	0.0	0.3	0.0	4.3	4.1	10.0	10.4
20	5/8 shackle	0.07	-0.65	0.45	0.0	0.3	0.0	4.1	3.5	10.4	12.4

21	3T Crosby Swivel	0.18	-4.17	0.33	0.0	0.3	0.0	3.5	1.1	12.4	115.4
22	5/8 shackle	0.07	-0.65	0.26	0.0	0.2	0.0	1.1	1.6	115.4	131.7
23	1/2 shackle	0.08	-0.30	0.30	0.0	0.2	0.0	1.6	1.9	131.7	137.5

4.6 Mooring Response

Buoys and moorings are placed in a very dynamic ocean environment and consequently have dynamic responses induced by ocean waves and currents. This section describes the static and dynamic response of the real-time mooring at Strawberry as evaluated by MDD.

4.6.1 Static Response

The real-time mooring at Strawberry Hill is not rigidly moored which makes it difficult to analyze. Instead, MDD solves for a static solution at an instant in time using an iterative process starting with a no flow condition as described in Section 4.5.2. The tension at the top and bottom of every element in the mooring is solved in MDD and listed similar to Table 5. MDD also gives the total tension on the anchor and its vertical and horizontal components.

4.6.2 Dynamic Response

The real-time mooring does have a dynamic response to ocean waves and currents, but MDD is unable to evaluate wave forces on moorings. For this analysis, waves were considered by evaluating the mooring at the instant it was at the crest of the 5-year wave calculated in Section 3.3. This was done by increasing the depth of water by half or the extreme wave height, H_5, or 3.4 m.

This is a valid evaluation since waves acting on buoys adds a resistance force, but this force is usually small and neglected (Randall, 1997). Inertia is not considered, nor is cable motion, vibration, snap loading, or strumming which may be an issue for devices with more complex shapes. Complex instruments may provide torque, twist a mooring, and have hydrodynamic lift, but none of these characteristics are considered here.

Since the solutions are all assumed to be locally static, a dynamic response is considered in the following two cases:

- **When the real-time mooring goes under water.** MDD predicts if the topmost surface float gets dragged under water by the currents and consequently gives a subsurface solution.
- **When the real-time mooring comes off the bottom.** The type of solution is also given as a subsurface solution, but MDD outputs, “Warning. Anchor is likely TOO light!” when the mooring is susceptible coming off the bottom and changing anchoring locations.

4.6.3 Modes of Failure

The three modes of failure considered for the real-time mooring are:

- **Functional failure** when the real-time mooring goes underwater. MDD will evaluate this case as a subsurface solution. In this situation, the datalogger's cable modem will be unable to transmit and the real-time mooring will not be fully meeting the intent of its design.
- **Physical failure** when the real-time comes off the bottom and the location of its anchor changes. MDD gives a subsurface solution again, but it additionally outputs, "Warning. Anchor is likely TOO light!"
- **Total failure** when the tension in a single element is too great and the component breaks due to point loading. This is evaluated by comparing the total tension on the anchor and the maximum tension in the mooring to the load rating of the weakest mooring element.

4.7 Mooring Results

The real-time mooring at Strawberry Hill was evaluated for various cases of expected site condition combinations. Table 6 shows the results of these MDD evaluations.

Table 6: Mooring evaluation results

Case	Starting Surface Current	Wind Velocity	Depth					Surface Solution	Surface Buoyancy Used	Physical Failure	Total Tension on Anchor	Maximum Tension in Mooring
			18.4 m	15 m	5 m	1 m	Bottom					
					Current							
	m/s	*m/s*	*m/s*	*m/s*	*m/s*	*m/s*	*m/s*	*Y/N*	*%*	*Y/N*	*kg*	*kg*
1	0.00			0.00	0.00	0.00	0.00	Y	14	N	1.6	1.6
2	0.17			0.17	0.17	0.07	0.00	Y	13	N	1.9	16.0
3	0.37			0.37	0.37	0.19	0.00	Y	13	N	4.0	16.3
4	0.37	-16.3		0.04	0.24	0.14	-0.03	Y	13	N	1.8	16.4
5	0.37	16.3 ⊥		0.37/0.33	0.37/0.13	0.19/0.05	0/0.03	Y	13	N	5.6	16.3
6	0.37	16.3		0.70	0.50	0.24	0.00	Y	24	N	12.8	24.1
7	0.90			0.90	0.90	0.46	0.00	N	100	N	80.5	90.4
8	0.95			0.95	0.95	0.49	0.00	N	100	Y	87.5	96.8
9	0.60	16.3		0.93	0.73	0.36	0.03	N	100	Y	82.2	92.1
10	0.60	16.3		0.93	0.73	0.36	0.03	N	100	Y	82.2	92.1
11	0.00		0.00		0.00	0.00	0.00	Y	14	N	1.4	16.7

12	0.37		0.37	0.37	0.19	0.00	Y	15	N	4.1	17.4
13	0.37	16.3	0.70	0.43	0.19	0.00	Y	74	N	40.3	53.7
14	0.75		0.75	0.75	0.39	0.00	N	100	N	62.8	75.0
15	0.95		0.95	0.95	0.49	0.00	N	100	Y	87.6	96.8
16	0.45	16.3	0.78	0.51	0.23	0.00	N	100	N	63.7	76.0
17	0.65	16.3	0.98	0.71	0.33	0.00	N	100	Y	83.4	93.1

* $\perp$ is wind perpendicular to current

* 0.37/0.33 is maximum current of 0.37 with perpendicular wind of 0.33 m/s

Table 5 is divided in to two sections and two subsections. The first section is the evaluations without waves, cases 1 through 10, at 15 m water depth. The second section is the evaluations with waves, cases 11 through 17, at 18.4 m water depth. Waves were considered by evaluating the mooring at the instant it was at the crest of the 5-year wave which was done by increasing the depth of water by half of the extreme wave height, H_5, or 3.4 m. These sections are subdivided into the expected extreme site condition evaluations and the failure evaluations. The expected extreme site condition cases are 1 through 6 without waves and 11 through 13 with waves. The failure cases are 7 through 10 without waves and 14 through 17 with waves.

Case 1 is evaluated with a zero velocity profile, case 2 with the mean velocity profile, and case 3 with the maximum velocity from Section 3.6. Since the case 3 had the greatest effect on the real-time mooring, it was used as the velocity profile for the remainder of the trials. In the failure cases where the velocity profile was increased till failure, the velocity profile at failure is still proportional to the maximum velocity profile from Section 3.6 where the surface current magnitude is the top 10 m of water and a bottom current magnitude is the current at a single location, 1 m from the bottom.

Cases 4, 5, and 6 are evaluated at the 5-year wind speed of 16.3 m/s from Section 3.7. The components of the wind velocity are automatically entered into the velocity profile, and cases 4, 5, and 6 are for current and wind velocities in opposing, perpendicular, and like directions respectively. Since the case 6 had the greatest effect on the real-time mooring, it was used as the extreme wind condition for the remainder of the trials. In the failure cases that included wind (9, 10, 16, and 17), the velocity profile was increased till failure, but the extreme wind speed was kept constant.

5 Construction

This section describes the materials, assembly, and testing, and ultimately the deployment of the real-time mooring at Strawberry Hill.

5.1 Materials

PISCO had originally procured the necessary materials for an ocean mooring but was never able to produce a fully functional real-time mooring. In the summer of 2007 an initial mooring was constructed to test the spar buoy. Once it was recovered in September 2007, it was stored in the Ship Ops compound as seen in Figure 17. These were the basic items available for the mooring construction.

Figure 17: Furnished materials

5.1.1 Spar Buoy

The spar buoy is 12 ft long and is centered vertically on a 4 in diameter steel tube as seen in Figure 18. Three links of anchor chain are welded to the bottom of the spar in order to lower the center of mass and create a righting moment. Spar buoys have the advantage of having good stability. Two foam-filled spheres have diameters of 2.5 ft and give the buoy its specified buoyancy of 250 lbs.

Figure 18: Furnished spar buoy

Spar buoys have a small buoyancy to drag ratio and are not as effective in providing the buoyancy required to support long mooring lines. However, when motion due to wave action must be suppressed, spar buoys are advantageous. Spar buoys are often moored from an auxiliary subsurface float which supports the bulk of the mooring line. Spar buoys of large dimension can provide heave and roll stability in most sea conditions (Berteaux, 1976).

5.1.2 Data Logger and Battery

Data logger, battery, and spar battery are shown in Figure 19. Each item has a diameter of 22.6 cm. The datalogger is 37.2 cm tall and each battery is 29.8 cm tall.

Figure 19: Datalogger, battery, and spare battery

Each item comes in a watertight pressure casing whose lid is secured with six Allen bolts and sealed with a greased O-ring. Inside the data logger casing is the actual datalogger and the cell phone modem. Inside the battery casing are four 6-volt lead acid batteries. These batteries must be charged in 12-volt pairs with a car battery charger. The datalogger weighs 15 lbs and each battery weighs 32 lbs. The combined equipment payload for the real-time mooring is 47 lbs.

The battery connects to the datalogger via a watertight power cord and the datalogger is connected to the instrument via a watertight, Kevlar-reinforced data cable as seen in Figure 20.

Figure 20: Data cable

Finally the datalogger and the cell phone transmissions are controlled by a software package called LoggerNet 3.4. The instrument has its own software to set its measurement interval, and it sends measurements to the datalogger as soon as it makes them. The datalogger stores this data until it is told by LoggerNet to transmit it to a designated IP address via the cell phone modem. The transmission is normally scheduled to occur daily but can also be done manually for instant access to instrument data. The software has some basic functionality to allow researchers to determine if their data sets are good and it can also report the level of the battery.

5.2 Assembly

This section describes the various construction processes that took place in order to prepare two moorings for a test in Yaquina Bay and an actual deployment at Strawberry Hill.

5.2.1 Spar Buoy Refurbishment

The provided spar buoy had a lot of surface corrosion as seen in Figure 21 and was in need of refurbishment.

Figure 21: Corroded buoy mounting plate

Halco Welding Inc. in South Beach, OR, was selected for the buoy refurbishment. The buoy was still at Ship Ops and Halco was willing to transport the buoy which negated any shipping expenses. The scope of work included sandblasting and painting services – see Appendix E. After sandblasting, Halco painted the buoy with yellow enamel paint as seen in Figure 22 and later with a brown, antifouling paint that prevents marine organisms from "bio-fouling" or adhering to the buoy.

Figure 22: Spar buoy painting at Halco Welding

5.2.2 Equipment Mount Fabrication

In order for the datalogger and its cell phone modem to work properly, it must remain above water on top of the spar buoy. The buoy has a mounting plate but there was no way of attaching the datalogger and battery to it. An equipment mount was needed to house the datalogger and battery and connect them to the buoy. In order to keep the center of gravity in line with the spar's vertical axis, the

equipment was stacked with the heavier battery on bottom in order to not raise the center of gravity any higher than necessary.

Megis Job Shop LCC in Corvallis, OR, was selected for the equipment mount fabrication. The scope of work required that the mount be kept as light as possible and that its weight remain evenly distributed around the spar's vertical axis– see Appendix F. The mount was welded from steel channels and included a top piece with drilled holes for the buoy light and 2 equipment stops for the data logger. Countersunk holes were drilled to attach the mount to the buoy and four 5/8" hex-head bolts.

Later the equipment mount was painted with primer and orange enamel. "OSU Zoology" and "541-737-8403" were stenciled on in black enamel paint and a final clear coat was applied as seen in Figure 23. The equipment mount weighs 83 lbs.

Figure 23: Painted equipment mount

5.2.3 Moorings

Separate moorings were constructed for Yaquina Bay and Strawberry Hill, but they both shared all the same components. All the wire rope segments were cut to size for each section of each mooring, and the remaining components were switched from one mooring to the other. Construction of the mooring lines took place on 22 and 23 August 2008 at the COAS compound on the OSU campus.

5.2.3.1 Yaquina Bay

The mooring for Yaquina Bay can be seen in Figure 24 and in Figure 25 below.

Figure 24: Entire view of Yaquina Bay mooring

Figure 25: Upper portion of Yaquina Bay mooring

5.2.3.2 Strawberry Hill

The mooring for Strawberry Hill can be seen in Figure 26 and in Figure 27 below.

Figure 26: Entire view of Strawberry Hill mooring

Figure 27: Upper portion of Strawberry Hill mooring

5.2.4 Cable Splicing

The watertight power cord that connects the battery to the datalogger was too short to reach the data logger from the desired stacked equipment position. Therefore, it had to be spiced by adding in an additional section of wire. This was done for both batteries.

The data cable also needed to be lengthened since it was only 20 m long. One option was to special order a 9 m extension for $161.50 from Sea-Bird Electronics, Inc. Another option was special order a 30

m cable for $637.50 from Sea-Bird Electronics, Inc. as well. It was decided to splice the existing, 20 m data cable with a spare 20 m data cable. Although the cable's tensile strength due to the Kevlar wrapping was lost, no additional money was spent and the project was not delayed because of a special order delivery time.

Both the power cord splice and the data cable splice required waterproofing measures. Each splice was individually shrink-wrapped. Then the entire bundle of wires was wrapped in a compressive puddy that forms a solid splice. Finally, the whole bundle of wires was taped and shrink-wrapped again.

5.3 Testing

Three separate field tests were performed on the real-time mooring. The first test was a pressure test for the datalogger and battery casings. The second test was a performance test of the spar buoy. The final test was an actual 1-week deployment of the real-time mooring at a site similar to Strawberry Hill.

5.3.1 Pool

The watertight pressure casings for the datalogger and batteries did not come with any sort of pressure rating. Since the equipment inside the datalogger is expensive, a leak in this casing would be disastrous. Any leaks in the battery casing leaks could allow the lead acid battery to get wet. If the battery reacts with the seawater it will produce a gas that can pressurize the casing, possibly to the point of explosion. For this reason a one-way valve was included in the casing's lid so that the battery casing can vent out gas in the event of a reaction. The pressure rating for the one-way valve is also unknown.

For the sake of safety, a pressure test was performed on 31 July 2008 at the Osborn Aquatic Center. The casing was taken down to the deepest part of the pool at 13 ft. The casing was oriented in all directions to look for leaks but no bubbles were detected. The next day, the casing was opened and there were no signs of moisture inside the casing. The desiccant card that was placed in the casing prior to the test showed only minor color change which can be attributed to the humidity of the air in the casing. Since the pressure casing and its one-way valve did not leak at 13 ft, it should be unaffected by ocean spray, splashing waves, or minor submersions.

5.3.2 Yaquina Bay

The performance of the spar buoy was tested on 27 August 2008 in Yaquina Bay. This location provided a more controlled environment to examine the heave and roll of the spar buoy with the new equipment mount. It also provided an opportunity to practice recovering the buoy from the R/V Elakha. Figure 28 and Figure 29 below show the initial steps of the Yaquina Bay test.

Figure 28: Fully Assembled mooring laid out on the pier

Figure 29: Tow straps connected to the buoy for crane lift

The mooring was deployed buoy first using the crane at Ship Ops and hoisting it from the pier to the water by the dock as seen in Figure 30 and Figure 31. The anchor chain was disconnected from the mooring and lowered second. Once at the surface of the water, it was reconnected to the mooring and released via quick release, since the water was rather shallow and there was no danger in having the anchor free fall.

Figure 30: Lowering the buoy into Yaquina Bay

Figure 31: Buoy and subsurface floats at Yaquina Bay

Once the mooring was in the water, it seemed perform well. The spar buoy did not list, which means the weight from the equipment mount had been evenly distributed. The distance between the center of gravity and the center of mass affects the buoy's "righting moment" or the ability to right itself. The

righting moment was investigated further by hand from the pier as seen in Figure 32. The buoy could not be tipped over by hand more than 45 degrees, and it righted itself immediately upon release.

The buoyancy was also investigated at Yaquina Bay. The spar buoy rode high in the water right at its painted waterline in the center of the top steel sphere. When forced by hand, the buoy could be submerged but only to the base of the equipment mount, and once released, it immediately returned to its waterline position. This test confirmed that the buoyancy from the buoy was sufficient. Finally, Kim Page-Albins and Daniel Lutz dove on the mooring to investigate the performance of the mooring under water as seen in Figure 33.

Figure 32: Testing the righting moment at Yaquina Bay

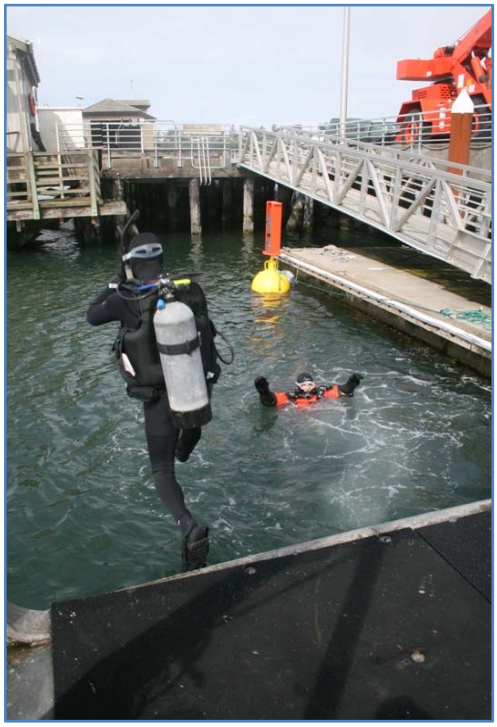

Figure 33: Diving on the mooring at Yaquina Bay

The S-shaped top line performed as designed by pulling the buoy and subsurface floats apart. The subsurface floats kept the lower section of the mooring line taut even with the movement of the spar buoy above. All connections from the bottom of the buoy all the way down to the anchor chain moved freely and kept from tangling. Finally, the divers attached a line to the anchor chain in preparation for the anchor first recovery by the R/V Elakha.

Afterwards, the entire mooring was successfully recovered using the winch and A-frame of the R/V Elakha. The anchor was brought onboard first. Next the mooring line and subsurface floats were pulled in by hand. Finally, the winch and A-frame were used to lift and pull the spar buoy onboard.

5.3.3 Wekonda Beach

The performance of the entire real-time mooring was tested on 11 September 2008 for one week at Wekonda Beach just north of Strawberry Hill. The site conditions are exactly the same as Strawberry Hill, but it is slightly closer to Newport and more accessible and cost effective for such a short deployment. This final test subjected the real-time mooring to the actual site conditions it will face at

Strawberry Hill for its 2009 summer-long deployment. The mooring team and the crew of the R/V Elakha were able to practice both deployment and recovery of the real-time mooring at sea. Finally, an instrument package was attached in order to test the logging and transmission ability of the datalogger.

The mooring team began assembly of the real-time mooring before sunrise and getting underway from Ship Ops. The equipment mount was attached to the buoy by four 5/8" hex-head bolts. The battery and datalogger were placed inside the equipment mount as seen in Figure 34, and they were secured by four stainless steel straps.

Figure 34: Installing equipment at the Ship Ops dock prior to departure

Once underway, the mooring team began the long task of securing the data cable all along the length of the mooring as seen in Figure 35. Any area of the data cable that was susceptible to chaffing was covered in plastic tubing. The idea is that the tubing will wear first, saving the data cable.

Figure 35: Preparing data cable while underway

Figure 36: Attaching instrument while underway

The data cable was connected from the datalogger to the instrument with its remaining slack coiled safely under the lowest subsurface float as seen in Figure 36. Finally it was attached to the mooring using plastic cable ties every half meter.

As the R/V Elakha arrived at Wekonda Beach, the real-time mooring was fully assembled and laid out on the deck. Since the deployment was buoy first, the mooring team attached a series of safety lines to the

spar buoy as seen in Figure 37. Next the buoy was hoisted into the water with the assistance of the R/V Elakha's A-frame and the hydraulic wench as seen in Figure 38.

Figure 37: Mooring team at the ready for deployment

Figure 38: Hoisting the buoy into the water

The safety lines were secured to the stern while the ship slowly trolled the buoy behind it as seen in Figure 39.

Figure 39: Buoy in the water at Wekonda Beach

Figure 39 clearly shows the Carmanah M501 solar-powered LED Marine lantern – see Appendix G. The M501 has a visibility of 1 nautical mile or 1.8 km. The color of the light is amber and it shines once every four seconds. Finally, the M501 has an IP68 certification for water ingress protection standards, and it meets the US Coast Guard 33CFR part 66 for PATONs.

The spar buoy was released from the safety lines and the mooring line was payed out by hand off the stern as seen in Figure 40. This allowed the instrument to be gently lowered into the water without risk of colliding with the stern. Finally, the anchor chain was hoisted into the water again with the assistance

of the R/V Elakha's A-frame and the hydraulic wench. It was then lowered into the water to approximately 5 m depth and released via quick release in order to not have the anchor free fall too far and avoid jerking the instrument into a collision with the anchor.

Figure 40: Paying out the mooring while trolling the buoy

Figure 41: Successful deployment of the real-time mooring

Once the mooring was in the water, it seemed to perform well. Again the buoy was not listing and it responded nicely to the small chop and ocean swell. The spar buoy rode high in the water right at its painted waterline in the center of the top steel sphere as seen in Figure 41. Water was observed to be splashing on the upper part of the buoy but not on the equipment mount. Unfortunately the conditions were not desirable for diving so the underwater performance of the mooring was not observed. From the surface, the S-shaped top line seemed to be doing its job and the buoy's motion was not restricted which suggests no tangles in the mooring line.

On 16 September 2008 the mooring team, without the author, attempted to recover the real-time mooring at Wekonda Beach. They dove on the mooring and attached a line to the anchor chain, but were unsuccessful at pulling in the spar buoy due to significant current and wind chop. A second attempt was made on 18 September 2008 and was successful. All equipment was intact and there was no damage to the spar buoy, the data cable, or the instrument.

6 Discussion

This section shows how the mooring will respond to the expected extreme site conditions at Strawberry Hill. It also describes three modes of failure that the real-time mooring may experience.

6.1 Extreme Conditions

MDD predicts that the real-time mooring at Strawberry Hill will have the greatest response to case 13. This prediction was expected since it represents the most extreme site conditions: Waves and Wind with Maximum Current. The mooring stayed above water, utilizing 74% of its buoyancy in this case, which means it should be able to successfully withstand all 5-year summer site conditions at Strawberry Hill. The entire MDD evaluation for case 13 is shown below and in Figure 42.

Height[m] U [m/s] V [m/s] W [m/s] Density [kg/m^3]
18.40 0.70 0.00 0.00 1024.00
5.00 0.43 0.00 0.00 1025.46
1.00 0.19 0.00 0.00 1025.89
0.00 0.00 0.00 0.00 1026.00

First, find neutral (no current) mooring component positions.
.....
Take a closer look at the convergence...
Depth Top Bottom % of float used delta-converge
18.4 21.8709 18.2109 16.3894 -0.001

This is (starting off as) a potential surface float mooring
Searching for a converged solution.
.....
This is a surface solution, using 74% of the surface buoyancy.
Total Tension on Anchor [kg] = 40.3
Vertical load [kg] = 26.0 Horizontal load [kg] = 30.8
Safe wet anchor mass = 116.0 [kg] = 255.3 [lb]
Safe dry steel anchor mass = 133.4 [kg] = 293.4 [lb]
Safe dry concrete anchor mass = 178.5 [kg] = 392.8 [lb]
Weight under anchor = -197.5 [kg] (negative is down)

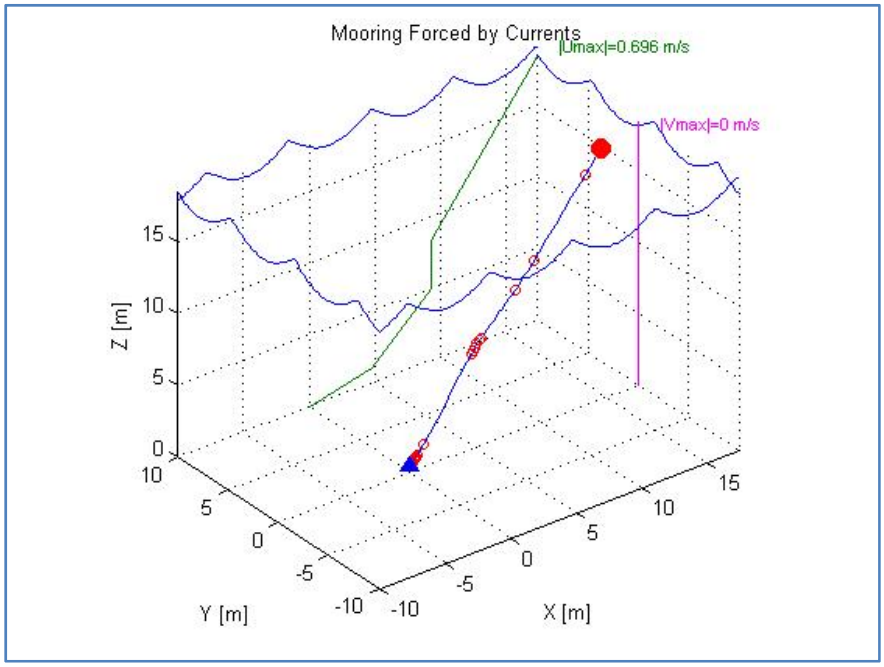

Figure 42: Mooring plot in waves and wind with maximum current

6.2 Functional failure

MDD was used to estimate the extreme environmental conditions that would lead to several cases of functional failure of the real-time mooring at Strawberry Hill. Functional failure is when the real-time

mooring goes underwater and the datalogger's cable modem will be unable to transmit information. An example of functional failure is case 7. The entire MDD evaluation for this case is shown below and in Figure 43.

Height[m]	*U [m/s]*	*V [m/s]*	*W [m/s]*	*Density [kg/m^3]*
15.00	*0.90*	*0.00*	*0.00*	*1024.00*
5.00	*0.90*	*0.00*	*0.00*	*1025.33*
1.00	*0.46*	*0.00*	*0.00*	*1025.87*
0.00	*0.00*	*0.00*	*0.00*	*1026.00*

First, find neutral (no current) mooring component positions.
.....
This is (starting off as) a potential surface float mooring
Searching for a converged solution.
.....
This is a sub-surface solution.
Total Tension on Anchor [kg] = 80.5
Vertical load [kg] = 38.0 Horizontal load [kg] = 71.0
Safe wet anchor mass = 234.4 [kg] = 515.7 [lb]
Safe dry steel anchor mass = 269.4 [kg] = 592.8 [lb]
Safe dry concrete anchor mass = 360.6 [kg] = 793.4 [lb]
Weight under anchor = -157.7 [kg] (negative is down)

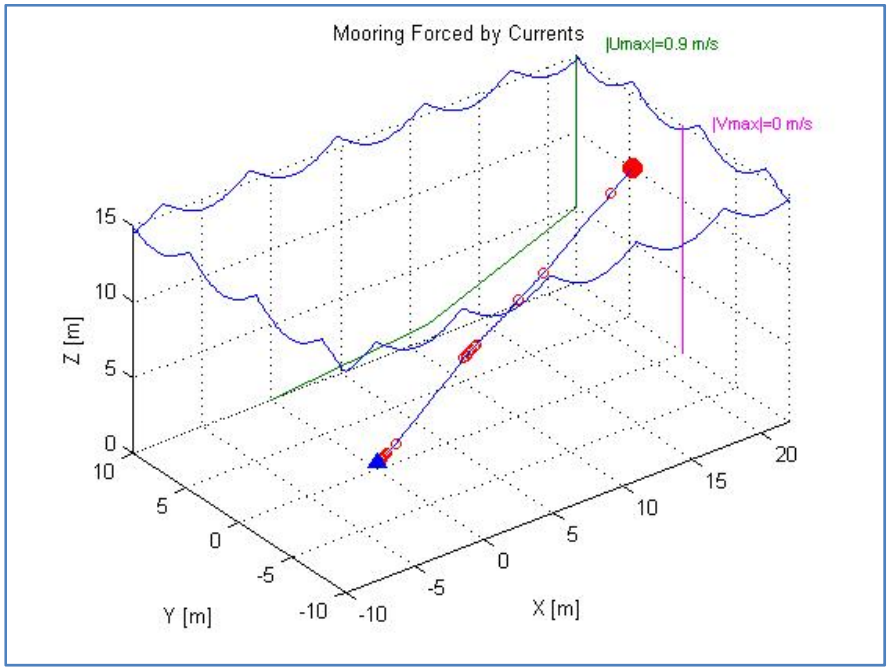

Figure 43: Mooring plot at functional failure

Case 7 above was not subjected to waves or wind and it failed functionally at a velocity profile where the surface current was 0.90 m/s. Case 14 was subjected to waves and current only and it failed

functionally when the surface current was 0.75 m/s. Finally, case 16 was subjected to wind, waves, and current and it failed functionally when the surface current was 0.45 m/s.

6.3 Physical Failure

MDD was used to estimate the extreme environmental conditions that would lead to several cases of physical failure of the real-time mooring at Strawberry Hill as well. Physical failure is when the real-time comes off the bottom and the location of its anchor changes. If the mooring moves to deeper water it may become submerged or it may become tangled in shallower water. In either case, the instrument will be collecting data at an unknown location and possibly an unknown depth. In the most severe case of functional failure, a mooring may be swept out to sea or washed up on a beach. An example of functional failure is case 17. The entire MDD evaluation for this case is shown below and in Figure 44.

Height[m]	*U [m/s]*	*V [m/s]*	*W [m/s]*	*Density [kg/m^3]*
18.40	*0.98*	*0.00*	*0.00*	*1024.00*
5.00	*0.71*	*0.00*	*0.00*	*1025.46*
1.00	*0.33*	*0.00*	*0.00*	*1025.89*
0.00	*0.00*	*0.00*	*0.00*	*1026.00*

First, find neutral (no current) mooring component positions.
..
This is (starting off as) a potential surface float mooring
Searching for a converged solution.
....
This is a sub-surface solution.
Total Tension on Anchor [kg] = 83.4
Vertical load [kg] = 38.5 Horizontal load [kg] = 73.9
Safe wet anchor mass = 242.6 [kg] = 533.7 [lb]
Safe dry steel anchor mass = 278.8 [kg] = 613.5 [lb]
Safe dry concrete anchor mass = 373.2 [kg] = 821.1 [lb]
Weight under anchor = -154.2 [kg] (negative is down)
!
!!*!* Warning. Anchor is likely TOO light!   *!*!*!*
!

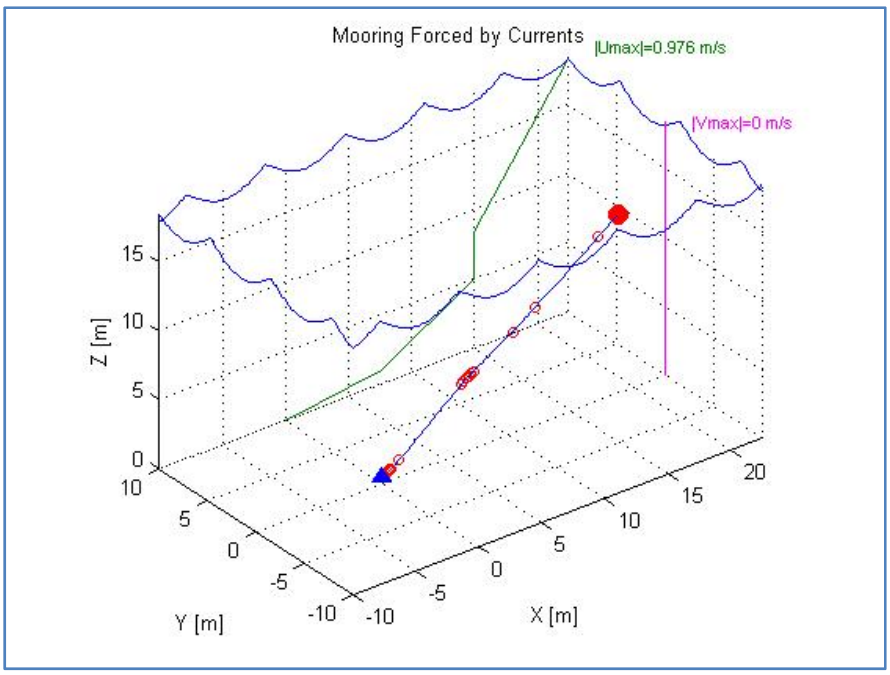

Figure 44: Mooring plot at physical failure in waves and wind

Case 17 above was subjected to waves and wind and it failed physically at a velocity profile where the surface current was 0.65 m/s. Case 15 was subjected to waves only and it failed physically at a velocity profile where the surface current was 0.95 m/s. Cases 10 and 9 were subjected to wind only and they failed both functionally and physically at a same velocity profile where the surface current was 0.60 m/s. Finally, case 8 was not subjected to waves or wind and it failed physically at a velocity profile where the surface current was 0.95 m/s.

6.4 Total Failure

Total failure is when the tension in a single element is too great and the component breaks due to point loading. This is evaluated by comparing the total tension on the anchor and the maximum tension in the mooring from Table 6 to the load rating from Table 4 of the 3/8 chain SL that is connected to the anchor and the 1/2 shackle that is the element at the point of maximum tension in every case.

From Section 6.1 Extreme Conditions, MDD predicts that the real-time mooring at Strawberry Hill will have the greatest response to expected extreme site conditions in case 13 – waves and wind with maximum current. For case 13, the factors of safety for total failure are as follows:

Load Limit of 3/8 chain SL ÷ Total Tension in the Anchor = 1191 kg ÷ 40.3 kg ≈ factor of 30

Load Limit of 1/2 shackle ÷ Maximum tension in Mooring = 1814 kg ÷ 53.7 kg ≈ factor of 34

From Section 6.3 Physical Failure, MDD predicts that the largest tensions in the real-time mooring are generated from case 17 – physical failure in waves and wind. For case 17, the factors of safety for total failure are as follows:

Load Limit of 3/8 chain SL ÷ Total Tension in the Anchor = 1191 kg ÷ 83.4 kg ≈ factor of 14

Load Limit of 1/2 shackle ÷ Maximum tension in Mooring = 1814 kg ÷ 93.1 kg ≈ factor of 19

Considering the calculated factors of safety for total failure above, it is unlikely that the real-time mooring at Strawberry Hill will fail due to point loading.

7 Conclusion

The project to design and construct a real-time ocean mooring at Strawberry Hill was a successful partnership between the Coastal and Ocean Engineering Program with the Department of Zoology at OSU. The mooring was soundly constructed for very little cost, and it successfully completed a one-week deployment at a location similar to the Strawberry Hill site. Finally, it was recovered safely with no damage, and is ready for a summer-long deployment to Strawberry Hill in 2009.

The analysis of the real-time mooring that followed its construction has confirmed its ability to withstand the most extreme summer site conditions. This section discusses the limits of the real-time mooring and its possible modes of failure. It contains final recommendations and potential areas of additional research for PISCO and any future researchers using the real-time mooring. Finally, it acknowledges the individuals who helped make this project successful.

7.1 Recommendations

It is recommended that the following current limits not be exceeded for the real-time mooring at Strawberry Hill:

- **Functional Failure**: At currents of 0.45 m/s or greater it can be expected that the real-time mooring may experience transmission errors due to occasional submersions.
- **Physical Failure**: At currents of 0.60 m/s or greater can be expected that the real-time mooring may come off the bottom and change anchoring locations. The position of the real-time mooring should be checked after such a storm event.
- **Total Failure**: Total failure for the real-time mooring did not occur under any of the tested conditions at Strawberry Hill.

Since the maximum surface current was 0.37 m/s from Section 3.6, the recommended current limits could be reached in a summer storm event. However these limits represent the “worst case scenario” of a 5-year wind in the direction of maximum current at the crest for a 5-year wave. These limits can be increased by adding more mass to the anchor to increase its weight and its resistance to being pulled off the bottom in strong currents.

The total failure recommendation above only considers point loading, but an ocean mooring is constantly loaded, unloaded, and reloaded. Fatigue was not considered in this analysis but it is highly recommended that the following maintenance be performed on the mooring.

- Replace chain and wire rope segments be replaced every two summers since they typically have a one-year lifespan.

- Replace the shackles and other hardware every five summers which is equivalent to a continuously used, two-year lifespan.

The spar buoy and equipment mount should also be repainted every year and their connecting hardware should be replaced every summer with high quality stainless steel fasteners to resist corrosion. Any area of the data cable that is susceptible to chaffing should be recovered in plastic tubing similar to the one-week deployment. Finally, the M501 marine lantern should operate up to 5 years maintenance free, but it should be tested each summer prior deployment of the real-time mooring.

7.2 Additional Research

The project to design and construct a real-time mooring at Strawberry Hill was successful but there are several areas of additional research that may be considered. The tensile loads of moorings deployed at sea for several months will vary from high values at the time of deployment/recovery and when submitted to strong environmental conditions, to low values in periods of calm weather and weak currents. MDD does not evaluate fatigue in the mooring, but further research should be considered in this area.

Additional research into better ways to incorporate wave loads, including wave induced velocities and accelerations, should be considered. Wave induced orbital velocities were calculated with magnitudes of 1.52 m/s at the surface down to 1.16 m/s at the bottom. This profile was linearly superimposed on the maximum current profile and then evaluated against the real-time mooring in MDD. The new, combined current profile was approximately six times as large at the maximum current profile, and it definitely gave a subsurface solution. The linearly superimposed method is an over-simplified way of including orbital velocities, and it should be reevaluated and refined. This project neglected dynamic loading and only analyzed the mooring statically at an instant in time. Dynamic forcing such as snap loading is not considered. Low-frequency dynamics (ex: “fishtailing”) induced by instability due to steady wind and current loads was also not considered.

MDD does not consider the strange occurrences that can happen at sea. A shackle can get turned sideways and be loaded in an unexpected direction. Tangles in the mooring line can also cause unexpected tensions. In the case of the real-time mooring at Strawberry Hill, if the S-shaped top line where to loop around the instrument at a low sea level condition, it could cause significant damage when the sea level rises and the mooring is subjected to with waves and current.

MDD does have the ability to calculate free fall speed, but it was never considered for the real-time mooring due to the shallow depth of water at Strawberry Hill. Fall speed may need to be considered if the real-time mooring is rebuilt for a location of greater depth while still using the same deployment method.

MDD also has the ability to predict elongation although none was found for the real-time mooring at Strawberry Hill. Again, if the real-time mooring is rebuilt for a location of greater depth and the mooring line is significantly longer or of another material, elongation should be considered.

7.3 Acknowledgements

I would like to sincerely thank the following groups and individuals who helped make this project success – your willingness is greatly appreciated.

- *Dr. Francis Chan* for allowing me to working on his PISCO team and funding the real-time mooring construction.
- *Dr. Sarah Dudas* for providing me with 2006 current data for Strawberry Hill.
- *Halco Welding Inc.* for their quality work on the spar buoy refurbishment and their willingness to transport it back and forth to Ship Ops – I could never have gotten that thing in my car!
- *Pete Megis of Megis Job Shop LCC* for his help in the design of the equipment mount, his quality fabrication, and his fellow service in the US Navy.
- *Nicolas Cropp* my 11-year-old neighbor that will do, as he admits, "anything for money" for his help with the construction of the mooring.
- *Grady Donathan* for his help with the pressure test and for lending me dive gear.
- *Jim Washburn* for his help with the pressure test and for lending me dive gear as well. Jim got me this contact for the PISCO project through his OSU Divers list serve.
- The *mooring team* and *R/V Elakha* crew consisting of:
    - *Tim Kehl* who helped with lots of heavy lifting.
    - *Carrie Craig* who photographed the at Yaquina Bay deployment.
    - *Mikal Davis* who photographed the Wekonda Beach deployment and processed my reimbursement.
    - *Rick Plummer* for working the wench on the R/V Elakha.
    - *Michael Kriz* for being a great skipper while onboard the R/V Elakha.
- *Dr. Solomon Yim* for his willingness to serve on my committee.
- *Dr. Daniel Cox* for his willingness to serve on my committee and his help in finding some initial references for buoy engineering.
- *Dr. Merrick Haller* for his time and patience as my major professor. I appreciate your flexibility with this project and your emphasis on weekly meetings – it really helped me get this done. Thank you very much for your thorough review of my project paper.
- *Walt Waldorf* for your time and patience with my countless questions about ocean moorings. I also appreciate you letting me do so much of my work at the COAS Compound – your tool shop is better than mine!
- *Kim Page-Albins* for impacting the project the most from first responding to Jim Washburn's email getting the buoy in the water – I could not have done it without your help.
- *Erin Lutz*, my wonderful bride, for her constant love and support. You are my biggest source of encouragement, and your willingness to let me spray paint a big, orange equipment mount in the front lawn all summer long, really tells me how much you love me!

8 References

Berteaux, H. O. (1976). *Buoy Engineering.* New York, Maryland: John Wiley & Sons.

Dewey, R. K. (2007, July 31). *Mooring Design & Dynamics.* Retrieved July 25, 2008, from Centre for Earth and Ocean Research, University of Victoria: http://canuck.seos.uvic.ca/rkd/mooring/moordyn.html

Goda, Y. (2000). Random Seas and Design of Maritime Structures. In Y. Goda, *Random Seas and Design of Maritime Structures* (pp. 377-425). Singapore: World Scientific.

National Data Buoy Center. (2008). Retrieved July 15, 2008, from National Oceanic and Atmospheric Administration: http://www.ndbc.noaa.gov

Randall, R. (1997). *Elements of Ocean Engineering.* New Jersey: Society of Naval Architects and Marine Engineers.

Tides and Currents. (2008). Retrieved July 15, 2008, from National Oceanic and Atmospheric Administration: http://www.co-ops.nos.noaa.gov/

9 Appendix

The following appendices are included in the report. Each section is labeled with its corresponding letter from the list below.

A. Calculation of 5-year Wave Height
B. Calculation of 5-year Wave Period
C. 2006 Current Data for Strawberry Hill
D. Calculation of 5-year Wind Speed
E. SOW: Buoy Refurbishment
F. SOW: Equipment Mount Fabrication
G. Carmanah M501 Solar-Powered LED Marine Lantern Specification

Peak significant wave heights of NDBC Buoy 46050

K=10 years, N=N $_T$ =82, λ =8.20, ν =1

Month	Hs (m)																														
January																															
February																															
March																															
April																															
May	6.0	5.5	5.5	5.5	5.5	5.5	5.5	5.5	5.5	5.5	5.5	5.5	5.5	5.0	5.0	5.0	5.0	5.0	5.0	5.0	5.0	5.0	5.0	5.0	5.0	5.0	5.0	5.0	5.0		
June	6.0	5.5	5.5	5.5	5.5	5.5	5.0	5.0	5.0	5.0	5.0	5.0	5.0	5.0	5.0	5.0	5.0	5.0													
July																															
August	5.0	5.0	5.0																												
September	7.5	7.0	7.0	6.5	6.5	6.5	6.5	6.5	6.0	6.0	6.0	6.0	5.5	5.5	5.5	5.5	5.5	5.0	5.0	5.0	5.0	5.0	5.0	5.0	5.0	5.0	5.0	5.0	5.0	5.0	5.0
October																															
November																															
December																															

Appendix A

N, N_T	82
K=	10
λ=	8.20
ν=	1

	Ahat	**Bhat**	k	α	β
FT-I	0.441	5.101	-	0.440	0.120
FT-II	0.383	5.098	10.0	0.492	0.109
Weilbull	0.844	4.592	1.4	0.428	0.394
Weilbull	1.189	4.299	2.0	0.391	0.363

m	x_m	FT-I		FT-II (k=10)		Weilbull (k=1.4)		Weilbull (k=2.0)	
		F_m	y_m	F_m	y_m	F_m	y_m	F_m	y_m
1	7.5	0.9932	4.985	0.9938	6.623	0.9931	3.144	0.9926	2.215
2	7.0	0.9810	3.954	0.9816	4.900	0.9809	2.672	0.9805	1.984
3	7.0	0.9688	3.452	0.9695	4.153	0.9688	2.430	0.9683	1.858
4	6.5	0.9566	3.116	0.9573	3.677	0.9566	2.264	0.9562	1.769
5	6.5	0.9445	2.862	0.9451	3.330	0.9445	2.135	0.9440	1.698
6	6.5	0.9323	2.658	0.9329	3.057	0.9324	2.030	0.9319	1.639
7	6.5	0.9201	2.486	0.9207	2.833	0.9202	1.940	0.9198	1.588
8	6.5	0.9079	2.337	0.9086	2.642	0.9081	1.862	0.9076	1.543
9	6.0	0.8958	2.207	0.8964	2.477	0.8960	1.792	0.8955	1.503
10	6.0	0.8836	2.089	0.8842	2.331	0.8838	1.729	0.8833	1.466
11	6.0	0.8714	1.983	0.8720	2.200	0.8717	1.672	0.8712	1.432
12	6.0	0.8592	1.886	0.8598	2.081	0.8596	1.619	0.8590	1.400
13	6.0	0.8471	1.796	0.8477	1.972	0.8474	1.570	0.8469	1.370
14	6.0	0.8349	1.712	0.8355	1.872	0.8353	1.524	0.8348	1.342
15	5.5	0.8227	1.634	0.8233	1.779	0.8231	1.481	0.8226	1.315
16	5.5	0.8105	1.560	0.8111	1.693	0.8110	1.440	0.8105	1.290
17	5.5	0.7983	1.491	0.7990	1.611	0.7989	1.401	0.7983	1.265
18	5.5	0.7862	1.425	0.7868	1.535	0.7867	1.365	0.7862	1.242
19	5.5	0.7740	1.362	0.7746	1.462	0.7746	1.329	0.7741	1.220
20	5.5	0.7618	1.302	0.7624	1.394	0.7625	1.296	0.7619	1.198
21	5.5	0.7496	1.244	0.7502	1.328	0.7503	1.264	0.7498	1.177
22	5.5	0.7375	1.189	0.7381	1.265	0.7382	1.233	0.7376	1.157
23	5.5	0.7253	1.136	0.7259	1.206	0.7261	1.203	0.7255	1.137
24	5.5	0.7131	1.084	0.7137	1.148	0.7139	1.174	0.7134	1.118
25	5.5	0.7009	1.035	0.7015	1.093	0.7018	1.146	0.7012	1.099
26	5.5	0.6887	0.986	0.6893	1.039	0.6896	1.119	0.6891	1.081
27	5.5	0.6766	0.940	0.6772	0.988	0.6775	1.092	0.6769	1.063
28	5.5	0.6644	0.894	0.6650	0.938	0.6654	1.067	0.6648	1.045
29	5.5	0.6522	0.850	0.6528	0.890	0.6532	1.042	0.6526	1.028
30	5.5	0.6400	0.807	0.6406	0.843	0.6411	1.018	0.6405	1.011
31	5.5	0.6279	0.765	0.6284	0.797	0.6290	0.994	0.6284	0.995
32	5.5	0.6157	0.724	0.6163	0.752	0.6168	0.971	0.6162	0.979
33	5.5	0.6035	0.683	0.6041	0.709	0.6047	0.948	0.6041	0.963

34	5.5	0.5913	0.644	0.5919	0.667	0.5925	0.926	0.5919	0.947
35	5.5	0.5792	0.605	0.5797	0.625	0.5804	0.904	0.5798	0.931
36	5.5	0.5670	0.567	0.5676	0.585	0.5683	0.883	0.5677	0.916
37	5.0	0.5548	0.529	0.5554	0.545	0.5561	0.862	0.5555	0.900
38	5.0	0.5426	0.492	0.5432	0.506	0.5440	0.841	0.5434	0.885
39	5.0	0.5304	0.456	0.5310	0.468	0.5319	0.821	0.5312	0.870
40	5.0	0.5183	0.420	0.5188	0.430	0.5197	0.801	0.5191	0.856
41	5.0	0.5061	0.384	0.5067	0.393	0.5076	0.782	0.5069	0.841
42	5.0	0.4939	0.349	0.4945	0.357	0.4955	0.762	0.4948	0.826
43	5.0	0.4817	0.314	0.4823	0.321	0.4833	0.743	0.4827	0.812
44	5.0	0.4696	0.280	0.4701	0.285	0.4712	0.725	0.4705	0.797
45	5.0	0.4574	0.246	0.4579	0.250	0.4590	0.706	0.4584	0.783
46	5.0	0.4452	0.212	0.4458	0.216	0.4469	0.688	0.4462	0.769
47	5.0	0.4330	0.178	0.4336	0.181	0.4348	0.670	0.4341	0.755
48	5.0	0.4208	0.144	0.4214	0.147	0.4226	0.652	0.4220	0.740
49	5.0	0.4087	0.111	0.4092	0.113	0.4105	0.634	0.4098	0.726
50	5.0	0.3965	0.078	0.3970	0.080	0.3984	0.617	0.3977	0.712
51	5.0	0.3843	0.045	0.3849	0.046	0.3862	0.599	0.3855	0.698
52	5.0	0.3721	0.012	0.3727	0.013	0.3741	0.582	0.3734	0.684
53	5.0	0.3600	-0.022	0.3605	-0.020	0.3619	0.565	0.3613	0.670
54	5.0	0.3478	-0.055	0.3483	-0.053	0.3498	0.548	0.3491	0.655
55	5.0	0.3356	-0.088	0.3362	-0.086	0.3377	0.531	0.3370	0.641
56	5.0	0.3234	-0.121	0.3240	-0.119	0.3255	0.514	0.3248	0.627
57	5.0	0.3113	-0.155	0.3118	-0.152	0.3134	0.497	0.3127	0.612
58	5.0	0.2991	-0.188	0.2996	-0.185	0.3013	0.481	0.3005	0.598
59	5.0	0.2869	-0.222	0.2874	-0.218	0.2891	0.464	0.2884	0.583
60	5.0	0.2747	-0.256	0.2753	-0.251	0.2770	0.447	0.2763	0.569
61	5.0	0.2625	-0.291	0.2631	-0.285	0.2649	0.431	0.2641	0.554
62	5.0	0.2504	-0.326	0.2509	-0.319	0.2527	0.414	0.2520	0.539
63	5.0	0.2382	-0.361	0.2387	-0.353	0.2406	0.398	0.2398	0.524
64	5.0	0.2260	-0.397	0.2265	-0.388	0.2284	0.381	0.2277	0.508
65	5.0	0.2138	-0.433	0.2144	-0.423	0.2163	0.365	0.2156	0.493
66	5.0	0.2017	-0.471	0.2022	-0.458	0.2042	0.348	0.2034	0.477
67	5.0	0.1895	-0.509	0.1900	-0.495	0.1920	0.332	0.1913	0.461
68	5.0	0.1773	-0.548	0.1778	-0.532	0.1799	0.315	0.1791	0.444
69	5.0	0.1651	-0.588	0.1656	-0.570	0.1678	0.298	0.1670	0.427
70	5.0	0.1529	-0.630	0.1535	-0.609	0.1556	0.281	0.1548	0.410
71	5.0	0.1408	-0.673	0.1413	-0.649	0.1435	0.264	0.1427	0.392
72	5.0	0.1286	-0.718	0.1291	-0.691	0.1314	0.247	0.1306	0.374
73	5.0	0.1164	-0.766	0.1169	-0.735	0.1192	0.229	0.1184	0.355
74	5.0	0.1042	-0.816	0.1048	-0.781	0.1071	0.211	0.1063	0.335
75	5.0	0.0921	-0.869	0.0926	-0.830	0.0949	0.193	0.0941	0.314
76	5.0	0.0799	-0.927	0.0804	-0.883	0.0828	0.174	0.0820	0.292
77	5.0	0.0677	-0.991	0.0682	-0.941	0.0707	0.155	0.0699	0.269
78	5.0	0.0555	-1.062	0.0560	-1.004	0.0585	0.135	0.0577	0.244
79	5.0	0.0434	-1.144	0.0439	-1.077	0.0464	0.113	0.0456	0.216
80	5.0	0.0312	-1.244	0.0317	-1.165	0.0343	0.091	0.0334	0.184
81	5.0	0.0190	-1.377	0.0195	-1.281	0.0221	0.066	0.0213	0.147
82	5.0	0.0068	-1.607	0.0073	-1.472	0.0100	0.037	0.0091	0.096
Correlation		r^2=	0.891	r^2=	0.914	r^2=	0.903	r^2=	0.846
5 Year Wave		y_5=	4.401	y_5=	4.479	y_5=	2.885	y_5=	2.099
		x_5=	7.042	x_5=	6.814	x_5=	7.027	x_5=	6.795

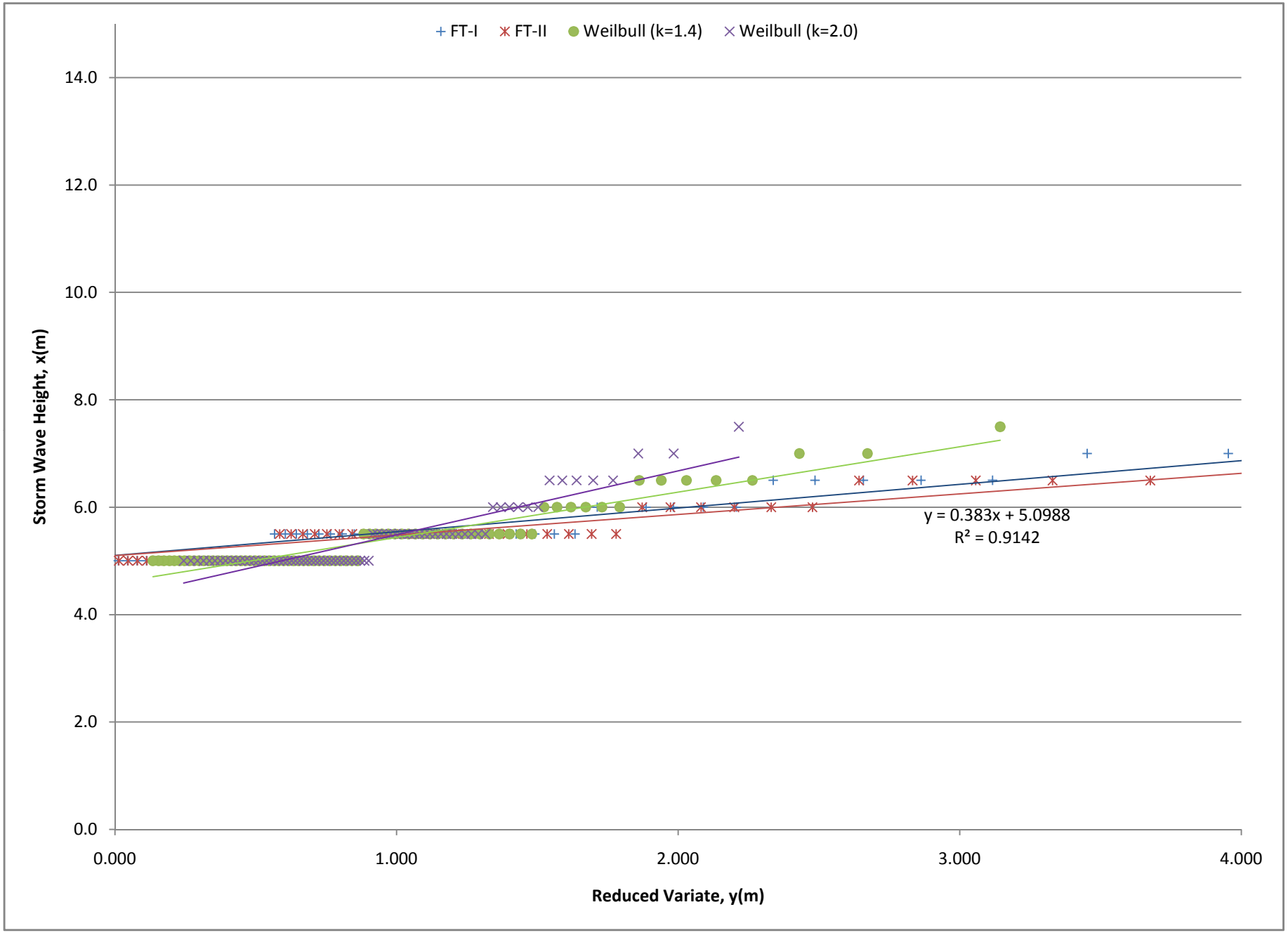
FT-I
FT-II
Weilbull (k=1.4)
Weilbull (k=2.0)
14.0
12.0
10.0
8.0
6.0
4.0
2.0
0.0
Storm Wave Height, x(m)
0.000
1.000
2.000
3.000
4.000
Reduced Variate, y(m)
y = 0.383x + 5.0988
R² = 0.9142

Peak significant wave periods of NDBC Buoy 46050

K=10 years, $N=N_T=110$, $\lambda=11.0$, $\nu=1$

Month	Hs (m)																																				
January																																					
February																																					
March																																					
April																																					
May	11.0	11.0	11.0	11.0	11.0	11.0	11.0	11.0	11.0	11.0	11.0	11.0	11.0																								
June	11.0	11.0	11.0	11.0	11.0	11.0	11.0	11.0																													
July																																					
August																																					
September	13.0	13.0	13.0	13.0	13.0	13.0	13.0	13.0	13.0	13.0	12.0	12.0	12.0	12.0	12.0	12.0	12.0	12.0	12.0	12.0	12.0	12.0	12.0	12.0	12.0	12.0	12.0	12.0	12.0	12.0	12.0	12.0	12.0	12.0	12.0	12.0	12.0
cont.	11.0	11.0	11.0	11.0	11.0	11.0	11.0	11.0	11.0	11.0	11.0	11.0	11.0	11.0	11.0	11.0	11.0	11.0	11.0	11.0	11.0	11.0	11.0	11.0	11.0	11.0	11.0	11.0	11.0	11.0	11.0	11.0	11.0	11.0	11.0	11.0	11.0
cont.	11.0	11.0	11.0	11.0	11.0	11.0	11.0	11.0	11.0	11.0	11.0	11.0	11.0	11.0	11.0																						
October																																					
November																																					
December																																					

N, N_T	110
K=	10
λ=	11.00
ν=	1

	Ahat	**Bhat**	k	α	β
FT-I	0.457	11.166	-	0.440	0.120
FT-II	0.398	11.156	10.0	0.492	0.109
Weilbull	0.904	10.603	1.4	0.428	0.394
Weilbull	1.242	10.327	2.0	0.391	0.363

m	x_m	FT-I		FT-II (k=10)		Weilbull (k=1.4)		Weilbull (k=2.0)	
		F_m	y_m	F_m	y_m	F_m	y_m	F_m	y_m
1	13.0	0.9949	5.279	0.9954	7.120	0.9948	3.275	0.9945	2.280
2	13.0	0.9858	4.250	0.9863	5.348	0.9858	2.812	0.9854	2.056
3	13.0	0.9768	3.750	0.9772	4.580	0.9767	2.575	0.9764	1.935
4	13.0	0.9677	3.415	0.9681	4.092	0.9676	2.412	0.9673	1.849
5	13.0	0.9586	3.163	0.9591	3.737	0.9586	2.287	0.9582	1.782
6	13.0	0.9495	2.960	0.9500	3.458	0.9495	2.185	0.9492	1.726
7	13.0	0.9404	2.790	0.9409	3.229	0.9405	2.098	0.9401	1.678
8	13.0	0.9313	2.643	0.9318	3.035	0.9314	2.022	0.9311	1.635
9	13.0	0.9223	2.514	0.9227	2.867	0.9224	1.955	0.9220	1.597
10	13.0	0.9132	2.399	0.9136	2.718	0.9133	1.894	0.9129	1.562
11	12.0	0.9041	2.295	0.9046	2.586	0.9042	1.839	0.9039	1.530
12	12.0	0.8950	2.199	0.8955	2.465	0.8952	1.788	0.8948	1.501
13	12.0	0.8859	2.111	0.8864	2.356	0.8861	1.741	0.8857	1.473
14	12.0	0.8769	2.029	0.8773	2.255	0.8771	1.697	0.8767	1.447
15	12.0	0.8678	1.953	0.8682	2.162	0.8680	1.655	0.8676	1.422
16	12.0	0.8587	1.882	0.8592	2.075	0.8589	1.616	0.8586	1.399
17	12.0	0.8496	1.814	0.8501	1.993	0.8499	1.579	0.8495	1.376
18	12.0	0.8405	1.750	0.8410	1.917	0.8408	1.544	0.8404	1.355
19	12.0	0.8315	1.690	0.8319	1.844	0.8318	1.511	0.8314	1.334
20	12.0	0.8224	1.632	0.8228	1.776	0.8227	1.479	0.8223	1.314
21	12.0	0.8133	1.577	0.8137	1.711	0.8137	1.449	0.8133	1.295
22	12.0	0.8042	1.524	0.8047	1.649	0.8046	1.419	0.8042	1.277
23	12.0	0.7951	1.473	0.7956	1.590	0.7955	1.391	0.7951	1.259
24	12.0	0.7861	1.424	0.7865	1.533	0.7865	1.364	0.7861	1.242
25	12.0	0.7770	1.377	0.7774	1.479	0.7774	1.337	0.7770	1.225
26	12.0	0.7679	1.331	0.7683	1.427	0.7684	1.312	0.7680	1.209
27	12.0	0.7588	1.287	0.7593	1.376	0.7593	1.287	0.7589	1.193
28	12.0	0.7497	1.245	0.7502	1.328	0.7502	1.263	0.7498	1.177
29	12.0	0.7406	1.203	0.7411	1.281	0.7412	1.240	0.7408	1.162
30	12.0	0.7316	1.163	0.7320	1.235	0.7321	1.218	0.7317	1.147
31	12.0	0.7225	1.124	0.7229	1.191	0.7231	1.195	0.7226	1.132
32	12.0	0.7134	1.086	0.7138	1.149	0.7140	1.174	0.7136	1.118
33	12.0	0.7043	1.048	0.7048	1.107	0.7050	1.153	0.7045	1.104

34	12.0	0.6952	1.012	0.6957	1.067	0.6959	1.133	0.6955	1.090
35	12.0	0.6862	0.976	0.6866	1.028	0.6868	1.113	0.6864	1.077
36	12.0	0.6771	0.942	0.6775	0.989	0.6778	1.093	0.6773	1.064
37	12.0	0.6680	0.908	0.6684	0.952	0.6687	1.074	0.6683	1.050
38	11.0	0.6589	0.874	0.6594	0.915	0.6597	1.055	0.6592	1.038
39	11.0	0.6498	0.842	0.6503	0.880	0.6506	1.037	0.6502	1.025
40	11.0	0.6408	0.809	0.6412	0.845	0.6415	1.018	0.6411	1.012
41	11.0	0.6317	0.778	0.6321	0.811	0.6325	1.001	0.6320	1.000
42	11.0	0.6226	0.747	0.6230	0.777	0.6234	0.983	0.6230	0.988
43	11.0	0.6135	0.716	0.6139	0.744	0.6144	0.966	0.6139	0.976
44	11.0	0.6044	0.686	0.6049	0.712	0.6053	0.949	0.6049	0.964
45	11.0	0.5954	0.657	0.5958	0.680	0.5962	0.933	0.5958	0.952
46	11.0	0.5863	0.627	0.5867	0.649	0.5872	0.916	0.5867	0.940
47	11.0	0.5772	0.599	0.5776	0.618	0.5781	0.900	0.5777	0.928
48	11.0	0.5681	0.570	0.5685	0.588	0.5691	0.884	0.5686	0.917
49	11.0	0.5590	0.542	0.5595	0.558	0.5600	0.869	0.5596	0.906
50	11.0	0.5499	0.514	0.5504	0.529	0.5510	0.853	0.5505	0.894
51	11.0	0.5409	0.487	0.5413	0.500	0.5419	0.838	0.5414	0.883
52	11.0	0.5318	0.460	0.5322	0.472	0.5328	0.823	0.5324	0.872
53	11.0	0.5227	0.433	0.5231	0.444	0.5238	0.808	0.5233	0.861
54	11.0	0.5136	0.406	0.5140	0.416	0.5147	0.793	0.5142	0.850
55	11.0	0.5045	0.380	0.5050	0.388	0.5057	0.779	0.5052	0.839
56	11.0	0.4955	0.353	0.4959	0.361	0.4966	0.764	0.4961	0.828
57	11.0	0.4864	0.327	0.4868	0.334	0.4875	0.750	0.4871	0.817
58	11.0	0.4773	0.302	0.4777	0.307	0.4785	0.736	0.4780	0.806
59	11.0	0.4682	0.276	0.4686	0.281	0.4694	0.722	0.4689	0.796
60	11.0	0.4591	0.251	0.4596	0.255	0.4604	0.708	0.4599	0.785
61	11.0	0.4501	0.225	0.4505	0.229	0.4513	0.694	0.4508	0.774
62	11.0	0.4410	0.200	0.4414	0.203	0.4423	0.681	0.4418	0.764
63	11.0	0.4319	0.175	0.4323	0.178	0.4332	0.667	0.4327	0.753
64	11.0	0.4228	0.150	0.4232	0.152	0.4241	0.654	0.4236	0.742
65	11.0	0.4137	0.125	0.4141	0.127	0.4151	0.641	0.4146	0.732
66	11.0	0.4046	0.100	0.4051	0.102	0.4060	0.628	0.4055	0.721
67	11.0	0.3956	0.075	0.3960	0.077	0.3970	0.615	0.3965	0.711
68	11.0	0.3865	0.051	0.3869	0.052	0.3879	0.602	0.3874	0.700
69	11.0	0.3774	0.026	0.3778	0.027	0.3788	0.589	0.3783	0.689
70	11.0	0.3683	0.001	0.3687	0.002	0.3698	0.576	0.3693	0.679
71	11.0	0.3592	-0.023	0.3597	-0.022	0.3607	0.563	0.3602	0.668
72	11.0	0.3502	-0.048	0.3506	-0.047	0.3517	0.550	0.3511	0.658
73	11.0	0.3411	-0.073	0.3415	-0.072	0.3426	0.538	0.3421	0.647
74	11.0	0.3320	-0.098	0.3324	-0.096	0.3336	0.525	0.3330	0.636
75	11.0	0.3229	-0.123	0.3233	-0.121	0.3245	0.513	0.3240	0.626
76	11.0	0.3138	-0.147	0.3142	-0.145	0.3154	0.500	0.3149	0.615
77	11.0	0.3048	-0.172	0.3052	-0.170	0.3064	0.488	0.3058	0.604
78	11.0	0.2957	-0.198	0.2961	-0.195	0.2973	0.475	0.2968	0.593
79	11.0	0.2866	-0.223	0.2870	-0.219	0.2883	0.463	0.2877	0.582
80	11.0	0.2775	-0.248	0.2779	-0.244	0.2792	0.450	0.2787	0.572
81	11.0	0.2684	-0.274	0.2688	-0.269	0.2701	0.438	0.2696	0.561
82	11.0	0.2594	-0.300	0.2598	-0.294	0.2611	0.426	0.2605	0.549
83	11.0	0.2503	-0.326	0.2507	-0.319	0.2520	0.413	0.2515	0.538
84	11.0	0.2412	-0.352	0.2416	-0.345	0.2430	0.401	0.2424	0.527
85	11.0	0.2321	-0.379	0.2325	-0.371	0.2339	0.389	0.2334	0.515
86	11.0	0.2230	-0.406	0.2234	-0.397	0.2249	0.376	0.2243	0.504

87	11.0	0.2139	-0.433	0.2143	-0.423	0.2158	0.364	0.2152	0.492
88	11.0	0.2049	-0.461	0.2053	-0.449	0.2067	0.352	0.2062	0.481
89	11.0	0.1958	-0.489	0.1962	-0.476	0.1977	0.339	0.1971	0.469
90	11.0	0.1867	-0.518	0.1871	-0.503	0.1886	0.327	0.1880	0.456
91	11.0	0.1776	-0.547	0.1780	-0.531	0.1796	0.314	0.1790	0.444
92	11.0	0.1685	-0.577	0.1689	-0.559	0.1705	0.302	0.1699	0.432
93	11.0	0.1595	-0.608	0.1599	-0.588	0.1614	0.289	0.1609	0.419
94	11.0	0.1504	-0.639	0.1508	-0.618	0.1524	0.276	0.1518	0.406
95	11.0	0.1413	-0.671	0.1417	-0.648	0.1433	0.264	0.1427	0.392
96	11.0	0.1322	-0.705	0.1326	-0.679	0.1343	0.251	0.1337	0.379
97	11.0	0.1231	-0.739	0.1235	-0.711	0.1252	0.238	0.1246	0.365
98	11.0	0.1141	-0.775	0.1144	-0.744	0.1162	0.224	0.1156	0.350
99	11.0	0.1050	-0.813	0.1054	-0.779	0.1071	0.211	0.1065	0.336
100	11.0	0.0959	-0.852	0.0963	-0.815	0.0980	0.197	0.0974	0.320
101	11.0	0.0868	-0.894	0.0872	-0.853	0.0890	0.184	0.0884	0.304
102	11.0	0.0777	-0.938	0.0781	-0.893	0.0799	0.169	0.0793	0.287
103	11.0	0.0687	-0.985	0.0690	-0.936	0.0709	0.155	0.0703	0.270
104	11.0	0.0596	-1.037	0.0599	-0.983	0.0618	0.140	0.0612	0.251
105	11.0	0.0505	-1.094	0.0509	-1.034	0.0527	0.125	0.0521	0.231
106	11.0	0.0414	-1.158	0.0418	-1.091	0.0437	0.109	0.0431	0.210
107	11.0	0.0323	-1.233	0.0327	-1.157	0.0346	0.092	0.0340	0.186
108	11.0	0.0232	-1.325	0.0236	-1.237	0.0256	0.074	0.0250	0.159
109	11.0	0.0142	-1.449	0.0145	-1.343	0.0165	0.054	0.0159	0.127
110	11.0	0.0051	-1.664	0.0055	-1.522	0.0075	0.030	0.0068	0.083
Correlation		r^2=	0.773	r^2=	0.779	r^2=	0.807	r^2=	0.756
5 Year Wave		y_5=	4.696	y_5=	4.916	y_5=	3.021	y_5=	2.168
		x_5=	13.310	x_5=	13.113	x_5=	13.335	x_5=	13.020

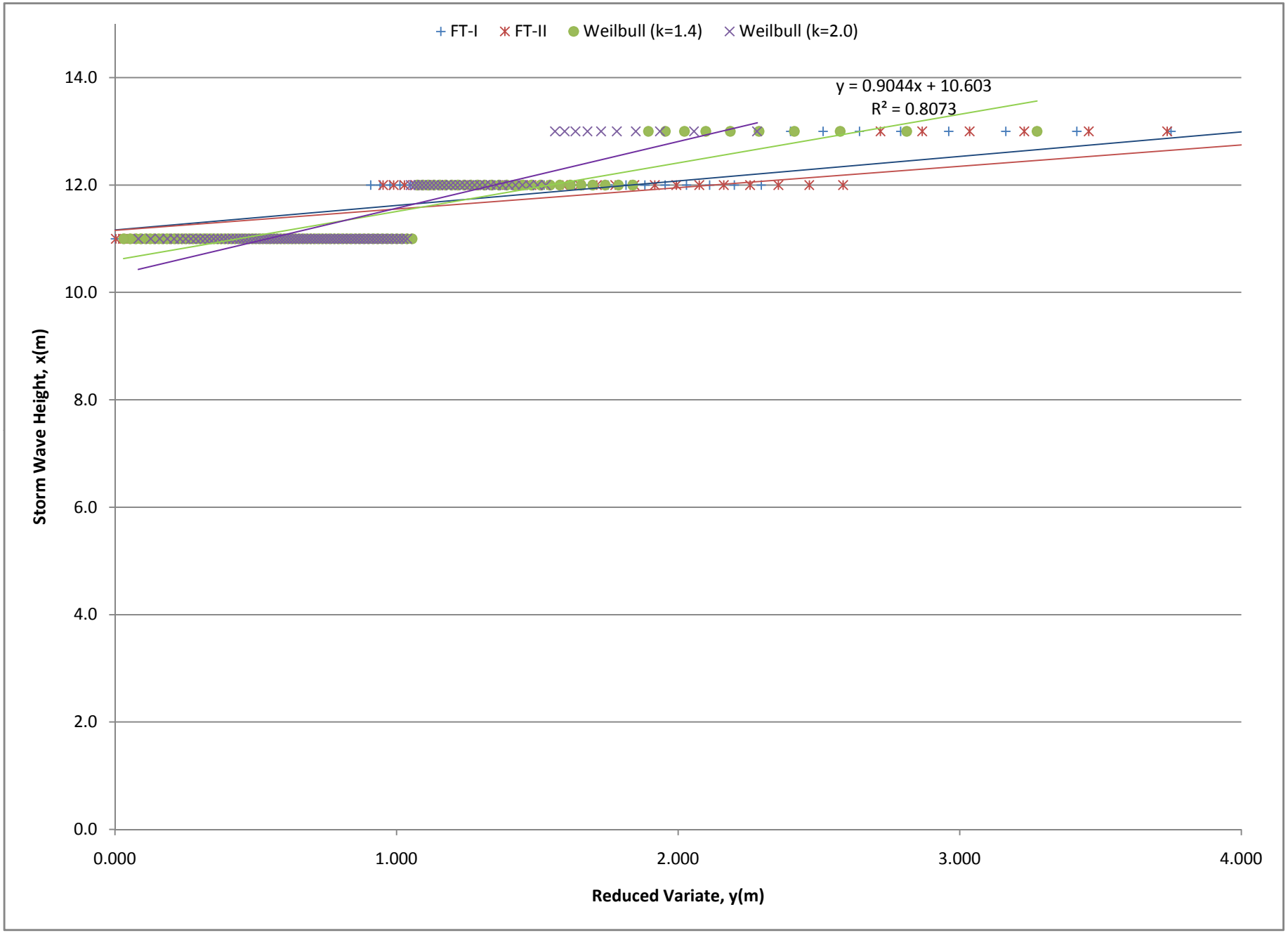
FT-I
FT-II
Weilbull (k=1.4)
Weilbull (k=2.0)
y = 0.9044x + 10.603
R² = 0.8073
14.0
12.0
10.0
8.0
6.0
4.0
2.0
0.0
Storm Wave Height, x(m)
0.000
1.000
2.000
3.000
4.000
Reduced Variate, y(m)

Surface velocity is for the top 10 meters of water with a reletively similar current
Bottom velocity is for the bottom layer of current

= max surface current

SH 06 *2006 Data for Strawberrry Hill*

Yearday	Julian Day	Date	SHUs (surface transport)	SHUb(bottom transport)	SHUbt(depth avged xshelf transport)	SHVbt(depth avgd alongshelf transport)	SHSxshelfvel (Surf xshelf velocity)	SHSalvel (Surf alongshore velocity)	Surface Magnitude (m/s)	SHBxshelfvel (Bott xshelf velocity)	SHBalvel (Bott alongshore velocity)	Bottom Magnitude (m/s)	Summed Magnitude (m/s)	
	150	31-May-06	0.088	-0.093	-0.0057	-0.1063	0.0071	-0.1848	0.1849	-0.031	-0.0353	0.0470	0.2319	
	151	1-Jun-06	-0.0201	0.0168	-0.0021	0.0493	-0.0146	0.0805	0.0818	-0.0073	0.0324	0.0332	0.1150	
	152	2-Jun-06	-0.0651	0.0672	-0.0008	0.2069	-0.0291	0.295	0.2964	0.0099	0.1304	0.1308	0.4272	
	153	3-Jun-06	-0.0107	0.0198	-0.0083	0.0316	-0.0211	0.0891	0.0916	-0.0044	-0.0061	0.0075	0.0991	
	154	4-Jun-06	-0.0303	0.0328	0.0022	0.1298	-0.0102	0.2152	0.2154	0.0054	0.0741	0.0743	0.2897	
	155	5-Jun-06	-0.0825	0.0428	0.0002	-0.0112	-0.0371	-0.05	0.0623	0.0019	0.0066	0.0069	0.0691	
	156	6-Jun-06	-0.0582	0.0242	0.0079	-0.1308	-0.0486	-0.2451	0.2499	0.0003	-0.0551	0.0551	0.3050	
	157	7-Jun-06	-0.0337	0.0274	0.0052	-0.131	-0.0358	-0.2565	0.2590	0.0007	-0.0478	0.0478	0.3068	
	158	8-Jun-06	0.0079	-0.0192	0.0036	-0.1435	-0.0312	-0.2401	0.2421	-0.0134	-0.0771	0.0783	0.3204	
	159	9-Jun-06	-0.0074	-0.0433	0.0078	-0.161	-0.0207	-0.256	0.2568	-0.0143	-0.0914	0.0925	0.3493	
	160	10-Jun-06	0.0115	-0.026	0.005	-0.1277	-0.0179	-0.2156	0.2163	-0.0117	-0.0634	0.0645	0.2808	
	161	11-Jun-06	-0.0432	0.0249	0.0006	-0.1344	-0.0328	-0.2463	0.2485	-0.0064	-0.0613	0.0616	0.3101	
	162	12-Jun-06	0.0154	-0.0256	-0.0039	-0.1219	-0.0019	-0.212	0.2120	-0.0135	-0.0527	0.0544	0.2664	
	163	13-Jun-06	0.0282	-0.0297	-0.0052	-0.0038	-0.0035	0.0452	0.0453	-0.014	-0.0197	0.0242	0.0695	
	164	14-Jun-06	0.0482	-0.0501	-0.0125	0.2773	-0.0038	0.3717	**0.3717**	-0.0219	0.1898	**0.1911**	**0.5628**	= max sum of 2 currents
	165	15-Jun-06	0.0955	-0.1016	-0.0138	0.2474	0.0073	0.3393	0.3394	-0.0344	0.1632	0.1668	0.5062	
	166	16-Jun-06	-0.0227	0.0094	-0.0055	0.1549	-0.0164	0.2381	0.2387	-0.0068	0.091	0.0913	0.3299	
	167	17-Jun-06	-0.0595	0.0392	-0.0048	-0.0079	-0.0318	-0.0424	0.0530	-0.0021	0.0111	0.0113	0.0643	
	168	18-Jun-06	-0.1065	0.0564	-0.0037	-0.1301	-0.0495	-0.2831	0.2874	-0.002	-0.034	0.0341	0.3215	
	169	19-Jun-06	-0.137	0.0969	0.0012	-0.0714	-0.05	-0.1923	0.1987	0.0127	-0.0152	0.0198	0.2185	
	170	20-Jun-06	-0.1052	0.098	-0.0005	-0.139	-0.0407	-0.25	0.2533	0.0099	-0.0697	0.0704	0.3237	
	171	21-Jun-06	-0.0562	0.0494	-0.0039	-0.1922	-0.0303	-0.3648	0.3661	0.0011	-0.0844	0.0844	0.4505	
	172	22-Jun-06	-0.0748	0.0776	-0.0016	-0.1838	-0.0248	-0.3283	0.3292	0.0091	-0.0815	0.0820	0.4112	
	173	23-Jun-06	-0.0941	0.0967	-0.0029	-0.1552	-0.0302	-0.2442	0.2461	0.0169	-0.0836	0.0853	0.3314	
	174	24-Jun-06	-0.0993	0.0993	-0.0046	-0.1521	-0.0334	-0.2023	0.2050	0.014	-0.1055	0.1064	0.3115	
	175	25-Jun-06	-0.084	0.0842	-0.003	-0.1257	-0.0305	-0.1705	0.1732	0.0132	-0.0896	0.0906	0.2638	
	176	26-Jun-06	-0.117	0.1171	-0.0089	-0.1308	-0.043	-0.1846	0.1895	0.0126	-0.0921	0.0930	0.2825	
	177	27-Jun-06	-0.1616	0.1615	-0.0092	-0.1763	-0.0506	-0.2433	0.2485	0.0251	-0.1194	0.1220	0.3705	
	178	28-Jun-06	-0.1102	0.1115	-0.0056	-0.1563	-0.039	-0.2001	0.2039	0.0155	-0.1191	0.1201	0.3240	
	179	29-Jun-06	-0.0906	0.0919	-0.0104	-0.0881	-0.034	-0.1212	0.1259	0.0094	-0.0598	0.0605	0.1864	
	180	30-Jun-06	-0.0562	0.0577	-0.0105	-0.1475	-0.0264	-0.1773	0.1793	0.0017	-0.1183	0.1183	0.2976	
	181	1-Jul-06	-0.0716	0.0725	-0.0035	-0.1594	-0.0225	-0.2158	0.2170	0.0112	-0.1125	0.1131	0.3300	
	182	2-Jul-06	-0.0653	0.0643	0.0039	-0.1037	-0.0182	-0.1543	0.1554	0.0136	-0.0632	0.0646	0.2200	
	183	3-Jul-06	-0.0202	0.0056	0.0036	-0.0674	-0.0085	-0.1278	0.1281	0.0019	-0.0258	0.0259	0.1540	
	184	4-Jul-06	-0.0629	0.0498	0.0054	-0.0424	-0.0231	-0.0871	0.0901	0.0072	-0.0205	0.0217	0.1118	
	191	11-Jul-06	0.12898	-0.11521	-0.00069569	0.0062969	0.018806	-0.026482	0.0325	-0.02718	0.019947	0.0337	0.0662	
	192	12-Jul-06	0.081494	-0.075133	-0.0045383	0.022124	0.013991	0.021782	0.0259	-0.022473	0.016958	0.0282	0.0540	
	193	13-Jul-06	0.02875	-0.047144	0.0044863	0.0058429	0.016386	0.016914	0.0235	-0.0080366	0.0076334	0.0111	0.0346	
	194	14-Jul-06	0.018789	-0.02099	-0.0041533	0.016642	-0.0041317	0.011377	0.0121	-0.011495	0.016973	0.0205	0.0326	
	195	15-Jul-06	0.0038788	-0.040709	-5.01E-05	-0.046556	-0.017666	-0.13229	0.1335	-0.017284	-0.0090362	0.0195	0.1530	
	196	16-Jul-06	-0.038656	-0.0054077	0.0071641	-0.12473	-0.014386	-0.22913	0.2296	-0.0013004	-0.061333	0.0613	0.2909	
	197	17-Jul-06	-0.065182	0.063983	0.0096504	-0.14774	-0.015751	-0.25072	0.2512	0.01574	-0.074513	0.0762	0.3274	
	198	18-Jul-06	-0.10614	0.10728	0.0075199	-0.10411	-0.021577	-0.17166	0.1730	0.026135	-0.05325	0.0593	0.2323	
	199	19-Jul-06	-0.091523	0.095517	0.0071965	-0.12704	-0.018138	-0.19734	0.1982	0.02312	-0.070195	0.0739	0.2721	
	200	20-Jul-06	-0.065869	0.068102	0.009105	-0.1585	-0.0084942	-0.24374	0.2439	0.020485	-0.085631	0.0880	0.3319	
	201	21-Jul-06	-0.022646	0.0040356	0.00082039	-0.10006	-0.012227	-0.17903	0.1794	-0.00016189	-0.048863	0.0489	0.2283	
	202	22-Jul-06	-0.071518	0.065235	-0.0053267	-0.11281	-0.023454	-0.18526	0.1867	0.0068528	-0.05677	0.0572	0.2439	
	203	23-Jul-06	-0.066643	0.057876	-0.0016833	-0.11085	-0.01165	-0.16555	0.1660	0.011208	-0.06813	0.0690	0.2350	
	204	24-Jul-06	-0.056438	0.056647	0.0030841	-0.16307	-0.0030818	-0.22952	0.2295	0.015366	-0.10403	0.1052	0.3347	
	205	25-Jul-06	-0.10076	0.097233	0.0077654	-0.17173	-0.017417	-0.23707	0.2377	0.02536	-0.11708	0.1198	0.3575	
	206	26-Jul-06	-0.062992	0.062499	0.0055918	-0.18177	-0.0074407	-0.22693	0.2271	0.017653	-0.14306	0.1441	0.3712	
	207	27-Jul-06	-0.10348	0.10359	0.0086183	-0.15873	-0.0098161	-0.21195	0.2122	0.030013	-0.11468	0.1185	0.3307	
	208	28-Jul-06	-0.026095	0.026679	0.0047759	-0.19374	-0.00044979	-0.26593	0.2659	0.0090177	-0.13315	0.1335	0.3994	
	209	29-Jul-06	0.026515	-0.033389	0.0066531	-0.16204	0.020179	-0.23282	0.2337	-0.0018843	-0.1034	0.1034	0.3371	
	210	30-Jul-06	0.017116	-0.014948	4.32E-05	-0.017095	-0.0027805	-0.046547	0.0466	-0.0034397	0.010862	0.0114	0.0580	
	211	31-Jul-06	-0.037181	0.042939	-0.0026869	0.066391	-0.022796	0.0059094	0.0235	0.0026872	0.064408	0.0645	0.0880	
	212	1-Aug-06	-0.10742	0.090358	0.0049197	-0.046009	-0.031636	-0.13511	0.1388	0.012744	-0.0020792	0.0129	0.1517	
	213	2-Aug-06	-0.02886	0.020303	0.0059065	-0.090875	0.00043913	-0.16853	0.1685	0.0079104	-0.034797	0.0357	0.2042	
	214	3-Aug-06	-0.068173	0.061581	0.0034227	-0.15637	-0.0088813	-0.21036	0.2105	0.016189	-0.10248	0.1038	0.3143	
	215	4-Aug-06	-0.044415	0.03692	0.002318	-0.19238	-0.0066979	-0.23805	0.2381	0.0091333	-0.1431	0.1434	0.3815	
	216	5-Aug-06	-0.068916	0.070817	0.0029755	-0.12078	-0.013619	-0.16213	0.1627	0.017501	-0.085315	0.0871	0.2498	
	217	6-Aug-06	-0.032161	0.03139	0.0067892	-0.17444	-0.0032504	-0.22596	0.2260	0.012397	-0.12571	0.1263	0.3523	
	218	7-Aug-06	-0.087995	0.088676	0.0060365	-0.1264	-0.014752	-0.1885	0.1891	0.021298	-0.082027	0.0847	0.2738	
	219	8-Aug-06	0.050119	-0.049578	-0.005151	0.037028	0.0046313	0.014853	0.0156	-0.013895	0.03155	0.0345	0.0500	
	220	9-Aug-06	-0.01632	0.019583	-0.0054362	0.068979	-0.010804	0.047119	0.0483	-0.0015742	0.066824	0.0668	0.1152	
	221	10-Aug-06	-0.059164	0.046558	0.0090901	-0.10757	-0.0048877	-0.169	0.1691	0.014047	-0.057999	0.0597	0.2287	
	222	11-Aug-06	-0.044672	0.035416	0.0034682	-0.076623	-0.010077	-0.12967	0.1301	0.0066614	-0.039623	0.0402	0.1702	
	223	12-Aug-06	-0.071135	0.068924	0.0050389	-0.12977	-0.017284	-0.18063	0.1815	0.016077	-0.087727	0.0892	0.2706	
	224	13-Aug-06	-0.042107	0.041679	0.0026771	-0.17269	-0.0038029	-0.19336	0.1934	0.011749	-0.1462	0.1467	0.3401	
	225	14-Aug-06	-0.089618	0.088712	0.0081362	-0.19524	-0.0078664	-0.24413	0.2443	0.024079	-0.15436	0.1562	0.4005	
	226	15-Aug-06	-0.07965	0.078245	0.0076951	-0.16104	-0.017695	-0.24075	0.2414	0.019585	-0.10674	0.1085	0.3499	
	227	16-Aug-06	-0.022914	0.021058	-0.00053752	-0.083971	-0.0072854	-0.16991	0.1701	-0.0012979	-0.032875	0.0329	0.2030	
	228	17-Aug-06	-0.078047	0.05102	0.0024295	-0.019474	-0.018469	-0.12575	0.1271	0.01015	0.031689	0.0333	0.1604	
	229	18-Aug-06	-0.045433	0.047784	0.0045405	-0.11469	-0.005195	-0.13978	0.1399	0.013342	-0.085976	0.0870	0.2269	
	230	19-Aug-06	-0.078478	0.070905	0.0015905	-0.12617	-0.020131	-0.16694	0.1681	0.013639	-0.098265	0.0992	0.2674	
	231	20-Aug-06	-0.037443	0.030474	0.0063319	-0.17045	-0.0046347	-0.24154	0.2416	0.013177	-0.11534	0.1161	0.3577	
	232	21-Aug-06	0.086311	-0.087475	0.007792	-0.042016	0.033646	-0.085254	0.0917	-0.0066131	-0.011933	0.0136	0.1053	
	233	22-Aug-06	-0.032295	0.019977	0.0033492	-0.004942	-0.009668	-0.062136	0.0629	0.0047807	0.023384	0.0239	0.0868	
	234	23-Aug-06	-0.076803	0.068684	0.0027403	-0.073491	-0.030461	-0.14523	0.1484	0.0087326	-0.026999	0.0284	0.1768	
	235	24-Aug-06	-0.098311	0.089659	0.006037	-0.13472	-0.021068	-0.2393	0.2402	0.019341	-0.061834	0.0648	0.3050	
	236	25-Aug-06	-0.058731	0.057565	0.0077734	-0.16019	-0.002989	-0.21495	0.2150	0.017522	-0.10368	0.1052	0.3201	
	237	26-Aug-06	-0.075452	0.075028	0.0023405	-0.17472	-0.0072655	-0.20804	0.2082	0.01887	-0.14122	0.1425	0.3506	
	238	27-Aug-06	-0.024027	0.018428	0.0015215	-0.1939	-0.00020955	-0.23326	0.2333	0.0056471	-0.15799	0.1581	0.3914	
	239	28-Aug-06	0.011465	-0.023042	0.0059027	-0.12464	0.007379	-0.17582	0.1760	0.00013812	-0.084085	0.0841	0.2601	
	240	29-Aug-06	0.012888	-0.038306	0.0028489	0.0083869	-0.0033361	-0.020151	0.0204	-0.009291	0.021152	0.0231	0.0435	
	241	30-Aug-06	0.02456	-0.015895	-0.0078575	0.048943	-0.0066641	0.012898	0.0145	-0.013446	0.042395	0.0445	0.0590	
	242	31-Aug-06	-0.084838	0.083083	0.0060635	-0.12458	-0.019547	-0.17515	0.1762	0.017946	-0.096314	0.0980	0.2742	
	243	1-Sep-06	0.0083286	-0.0095036	0.0095388	-0.041136	0.0041678	-0.062389	0.0625	0.00056342	-0.021081	0.0211	0.0836	
	244	2-Sep-06	0.17905	-0.16317	-0.0071803	-0.068293	0.038971	-0.077017	0.0863	-0.040771	-0.039431	0.0567	0.1430	
	245	3-Sep-06	-0.051131	0.022183	0.003162	-0.066048	-0.02175	-0.098994	0.1014	0.002215	-0.03617	0.0362	0.1376	
	246	4-Sep-06	-0.078295	0.066198	0.0073857	-0.089359	-0.027178	-0.20416	0.2060	0.013097	-0.012175	0.0179	0.2238	
	247	5-Sep-06	-0.1077	0.083134	0.0038746	-0.11873	-0.022456	-0.20504	0.2063	0.019306	-0.053717	0.0571	0.2633	
	248	6-Sep-06	-0.037359	0.039401	0.009339	-0.15644	0.0052118	-0.2091	0.2092	0.017478	-0.10551	0.1069	0.3161	
	249	7-Sep-06	-0.033494	0.038092	0.010306	-0.16872	0.0019305	-0.23932	0.2393	0.017049	-0.10468	0.1061	0.3454	
	250	8-Sep-06	-0.045045	0.035366	0.0054231	-0.096686	-0.014574	-0.1448	0.1455	0.0097263	-0.056038	0.0569	0.2024	
									0.1773	mean surface & bottom current		0.0727		

Appendix C

Peak significant wind speeds of NDBC Buoy 46050

K=10 years, N=N $_T$ =84, λ =8.4, ν =1

Month	Vs (knots)																												
January																													
February																													
March																													
April																													
May	31	30	29	29	29	29	28	28	28	28	27	27	26	26	26	26	26	26	26	26	26	26							
June	30	29	28	28	28	28	28	28	28	28	28	27	27	27	27	27	27	27	27	27	26	26	26	26	26	26	26	26	26
July	27	27	26																										
August	26																												
September	32	31	30	30	30	29	29	29	28	28	28	28	28	27	27	27	27	27	26	26	26	26	26	26	26	26	26	26	26
October																													
November																													
December																													

Appendix D

N, N_T	84
K=	10
λ=	8.4
ν=	1

	Ahat	**Bhat**	k	α	β
FT-I	1.109	26.724	-	0.440	0.120
FT-II	0.963	26.701	10.0	0.492	0.109
Weilbull	2.170	25.380	1.4	0.428	0.394
Weilbull	3.036	24.667	2.0	0.391	0.363

m	x_m	FT-I		FT-II (k=10)		Weilbull (k=1.4)		Weilbull (k=2.0)	
		F_m	y_m	F_m	y_m	F_m	y_m	F_m	y_m
1	32	0.9933	5.009	0.9940	6.664	0.9932	3.154	0.9928	2.221
2	31	0.9815	3.978	0.9821	4.937	0.9814	2.684	0.9809	1.990
3	31	0.9696	3.477	0.9702	4.187	0.9695	2.442	0.9691	1.864
4	30	0.9577	3.141	0.9583	3.711	0.9577	2.276	0.9572	1.775
5	30	0.9458	2.887	0.9464	3.363	0.9458	2.148	0.9454	1.705
6	30	0.9339	2.683	0.9345	3.089	0.9340	2.042	0.9335	1.646
7	30	0.9220	2.511	0.9226	2.865	0.9221	1.953	0.9217	1.596
8	30	0.9101	2.363	0.9107	2.674	0.9103	1.875	0.9098	1.551
9	29	0.8982	2.232	0.8988	2.509	0.8984	1.806	0.8980	1.511
10	29	0.8864	2.115	0.8870	2.362	0.8866	1.743	0.8861	1.474
11	29	0.8745	2.009	0.8751	2.231	0.8747	1.686	0.8742	1.440
12	29	0.8626	1.912	0.8632	2.112	0.8629	1.633	0.8624	1.408
13	29	0.8507	1.822	0.8513	2.004	0.8510	1.584	0.8505	1.379
14	29	0.8388	1.739	0.8394	1.904	0.8392	1.538	0.8387	1.351
15	29	0.8269	1.660	0.8275	1.811	0.8273	1.495	0.8268	1.324
16	29	0.8150	1.587	0.8156	1.724	0.8155	1.455	0.8150	1.299
17	28	0.8031	1.518	0.8037	1.643	0.8036	1.416	0.8031	1.275
18	28	0.7913	1.452	0.7918	1.566	0.7918	1.380	0.7913	1.252
19	28	0.7794	1.389	0.7800	1.494	0.7799	1.345	0.7794	1.229
20	28	0.7675	1.329	0.7681	1.425	0.7681	1.311	0.7676	1.208
21	28	0.7556	1.272	0.7562	1.360	0.7562	1.279	0.7557	1.187
22	28	0.7437	1.217	0.7443	1.297	0.7444	1.248	0.7439	1.167
23	28	0.7318	1.164	0.7324	1.237	0.7325	1.219	0.7320	1.148
24	28	0.7199	1.113	0.7205	1.180	0.7207	1.190	0.7201	1.128
25	28	0.7080	1.063	0.7086	1.125	0.7088	1.162	0.7083	1.110
26	28	0.6961	1.016	0.6967	1.071	0.6970	1.135	0.6964	1.092
27	28	0.6843	0.969	0.6848	1.020	0.6851	1.109	0.6846	1.074
28	28	0.6724	0.924	0.6729	0.970	0.6733	1.083	0.6727	1.057
29	28	0.6605	0.880	0.6611	0.922	0.6614	1.059	0.6609	1.040
30	28	0.6486	0.837	0.6492	0.875	0.6496	1.035	0.6490	1.023
31	28	0.6367	0.795	0.6373	0.830	0.6378	1.011	0.6372	1.007
32	28	0.6248	0.754	0.6254	0.786	0.6259	0.988	0.6253	0.991
33	28	0.6129	0.714	0.6135	0.743	0.6141	0.966	0.6135	0.975

34	28	0.6010	0.675	0.6016	0.700	0.6022	0.944	0.6016	0.959
35	27	0.5892	0.637	0.5897	0.659	0.5904	0.922	0.5898	0.944
36	27	0.5773	0.599	0.5778	0.619	0.5785	0.901	0.5779	0.929
37	27	0.5654	0.562	0.5659	0.580	0.5667	0.880	0.5661	0.914
38	27	0.5535	0.525	0.5541	0.541	0.5548	0.860	0.5542	0.899
39	27	0.5416	0.489	0.5422	0.503	0.5430	0.840	0.5423	0.884
40	27	0.5297	0.453	0.5303	0.466	0.5311	0.820	0.5305	0.870
41	27	0.5178	0.418	0.5184	0.429	0.5193	0.801	0.5186	0.855
42	27	0.5059	0.384	0.5065	0.393	0.5074	0.781	0.5068	0.841
43	27	0.4941	0.349	0.4946	0.357	0.4956	0.763	0.4949	0.826
44	27	0.4822	0.315	0.4827	0.322	0.4837	0.744	0.4831	0.812
45	27	0.4703	0.282	0.4708	0.287	0.4719	0.726	0.4712	0.798
46	27	0.4584	0.248	0.4589	0.253	0.4600	0.708	0.4594	0.784
47	27	0.4465	0.215	0.4471	0.219	0.4482	0.690	0.4475	0.770
48	27	0.4346	0.182	0.4352	0.186	0.4363	0.672	0.4357	0.756
49	27	0.4227	0.150	0.4233	0.152	0.4245	0.655	0.4238	0.743
50	27	0.4108	0.117	0.4114	0.119	0.4126	0.637	0.4120	0.729
51	27	0.3990	0.085	0.3995	0.086	0.4008	0.620	0.4001	0.715
52	27	0.3871	0.052	0.3876	0.054	0.3889	0.603	0.3882	0.701
53	26	0.3752	0.020	0.3757	0.021	0.3771	0.586	0.3764	0.687
54	26	0.3633	-0.012	0.3638	-0.011	0.3652	0.569	0.3645	0.673
55	26	0.3514	-0.045	0.3519	-0.043	0.3534	0.553	0.3527	0.659
56	26	0.3395	-0.077	0.3400	-0.075	0.3415	0.536	0.3408	0.646
57	26	0.3276	-0.110	0.3282	-0.108	0.3297	0.520	0.3290	0.632
58	26	0.3157	-0.142	0.3163	-0.140	0.3178	0.503	0.3171	0.618
59	26	0.3039	-0.175	0.3044	-0.172	0.3060	0.487	0.3053	0.604
60	26	0.2920	-0.208	0.2925	-0.204	0.2941	0.471	0.2934	0.589
61	26	0.2801	-0.241	0.2806	-0.237	0.2823	0.455	0.2816	0.575
62	26	0.2682	-0.275	0.2687	-0.269	0.2704	0.438	0.2697	0.561
63	26	0.2563	-0.309	0.2568	-0.302	0.2586	0.422	0.2579	0.546
64	26	0.2444	-0.343	0.2449	-0.336	0.2467	0.406	0.2460	0.531
65	26	0.2325	-0.378	0.2330	-0.369	0.2349	0.390	0.2342	0.516
66	26	0.2206	-0.413	0.2212	-0.403	0.2230	0.374	0.2223	0.501
67	26	0.2087	-0.449	0.2093	-0.437	0.2112	0.358	0.2104	0.486
68	26	0.1969	-0.486	0.1974	-0.473	0.1993	0.342	0.1986	0.471
69	26	0.1850	-0.523	0.1855	-0.508	0.1875	0.325	0.1867	0.455
70	26	0.1731	-0.562	0.1736	-0.545	0.1756	0.309	0.1749	0.438
71	26	0.1612	-0.602	0.1617	-0.582	0.1638	0.292	0.1630	0.422
72	26	0.1493	-0.643	0.1498	-0.621	0.1519	0.276	0.1512	0.405
73	26	0.1374	-0.685	0.1379	-0.661	0.1401	0.259	0.1393	0.387
74	26	0.1255	-0.730	0.1260	-0.702	0.1282	0.242	0.1275	0.369
75	26	0.1136	-0.777	0.1141	-0.746	0.1164	0.225	0.1156	0.351
76	26	0.1018	-0.826	0.1023	-0.791	0.1045	0.207	0.1038	0.331
77	26	0.0899	-0.879	0.0904	-0.840	0.0927	0.189	0.0919	0.310
78	26	0.0780	-0.937	0.0785	-0.892	0.0808	0.171	0.0801	0.289
79	26	0.0661	-0.999	0.0666	-0.949	0.0690	0.152	0.0682	0.266
80	26	0.0542	-1.070	0.0547	-1.012	0.0571	0.132	0.0563	0.241
81	26	0.0423	-1.151	0.0428	-1.084	0.0453	0.111	0.0445	0.213
82	26	0.0304	-1.251	0.0309	-1.171	0.0334	0.089	0.0326	0.182
83	26	0.0185	-1.383	0.0190	-1.286	0.0216	0.065	0.0208	0.145
84	26	0.0067	-1.612	0.0071	-1.477	0.0097	0.037	0.0089	0.095
Correlation		r^2=	0.934	r^2=	0.931	r^2=	0.953	r^2=	0.926
5 Year Wind		y_5=	4.425	y_5=	4.515	y_5=	2.896	y_5=	2.105
		x_5=	31.629	x_5=	31.049	x_5=	31.665	x_5=	31.057

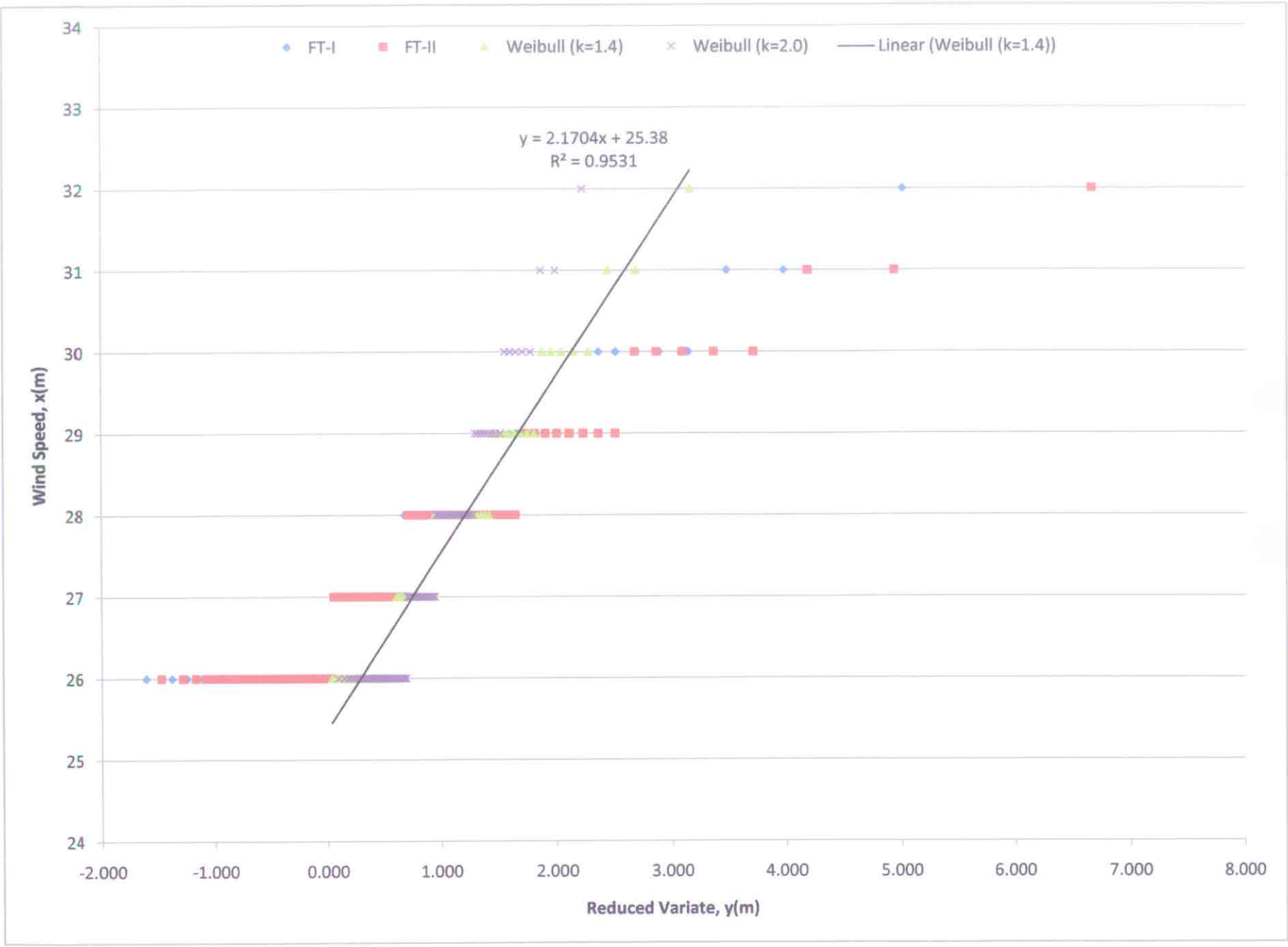
FT-I
FT-II
Weibull (k=1.4)
Weibull (k=2.0)
Linear (Weibull (k=1.4))
y = 2.1704x + 25.38
R² = 0.9531
Wind Speed, x(m)
Reduced Variate, y(m)
34
33
32
31
30
29
28
27
26
25
24
-2.000
-1.000
0.000
1.000
2.000
3.000
4.000
5.000
6.000
7.000
8.000

Appendix D

Project	Send Invoice to
Oregon State University Spar Buoy	Zoology Department
	3029 Cordley Hall
Point of Contact	Corvallis, OR 97331
Daniel Lutz	Attn: Mary Crafts
541-602-5020	Index #: F0517A

Scope of Work

1. Sandblasting
    a. If possible, first separate spar buoy into two pieces by removing center bolt as shown in photo below. (Replace center bolt if needed.)

    b. Sandblast all pieces to remove all paint and corrosion.
2. Welding
    a. Weld on a new "cable guide" parallel to the buoy floats, but not touching (floats have a foam center that welding can damage) as shown in photo below.

3. Painting
    a. Reassemble spar buoy and prime.
    b. Paint the upper portion of the buoy and top float yellow and the remainder of the buoy with paint resistant to bio-fouling as shown in photo above.

Project	Send Invoice to
Oregon State University Equipment Mount	Zoology Department
	3029 Cordley Hall
Point of Contact	Corvallis, OR 97331
Daniel Lutz	Attn: Mary Crafts
541-602-5020	Index #: F0517A

Scope of Work

1. Fabricate a mount for the following pieces of equipment:
    a. Data logger (included)
    b. Battery (included)
    c. Light (not included
2. See attached drawing for mount dimensions
3. Use sample buoy mount to match and drill equipment mount
4. Keep the mount as light as possible and the weight evenly distributed around the buoy's central axis.

Figure 1: Sample mount for reference

Carmanah®

MODEL

M501

Solar-Powered LED Marine Lanterns

Carmanah's world renowned Model M501 solar marine lantern offers excellent value and extremely reliable operation for up to 5 years. With a virtually indestructible design, the Model M501 solar marine lantern is completely waterproof, vibration proof and vandal resistant.

LIGHT OUTPUT AND OPERATION	
Visibility[1,2]	1 nautical mile (1.8 kilometers)
Peak intensity (360-degree average, green LEDs)	~1.2 Candela
IP68 waterproof rating	Yes
Temperature range	-40° to +176° F (-40° to +80° C)
Autonomy (flashing) at full charge	300 hrs
Horizontal output	360°
Available LED color	Red, green, amber or white
Colored lens option	Red lens only, flashing only, and manual switch model only
Flash patterns	7
CONSTRUCTION	
Solar panels	Mono-crystalline potted with UV-protected polyurethane and domed for higher efficiency
Light source	LED
Lifespan of LEDs	Up to 100,000 hours
Lens material	Polycarbonate
Battery (average 5-year life)	Non-replaceable
Battery amp-hour	2.5Ah
Battery venting	Vent at the bottom of the lantern
Sealing	Self-contained unit, potted with polyurethane
MICROSOURCE®	No
Scheduled maintenance	None for 5 years
Mounting options	2 Bolt
Weight	2.45 lbs (1.1 kg)
TRADEMARKS, PATENTS AND APPROVALS	
WEEE compliant	Yes
RoHS compliant	Yes
CE Approval	As per EN 60945:1997
Trademarks and Patents	US Patents: 6,573,659 and 6,013,985 Other Patents Pending

Distributed in USA by:
Premier Materials
7401 Central Ave NE
Minneapolis, MN 55432
800-262-2275
763-785-1509
www.premiermaterials.com

CHANGE THE WORLD WITH US™

Carmanah Technologies Corp. • Tel: +1.250.380.0052 • Fax: +1.250.380.0062 • E-mail: info@solarmarinelights.com • carmanah.com

Solar-Powered LED Marine Lanterns
Model M501

Carmanah®

Side View

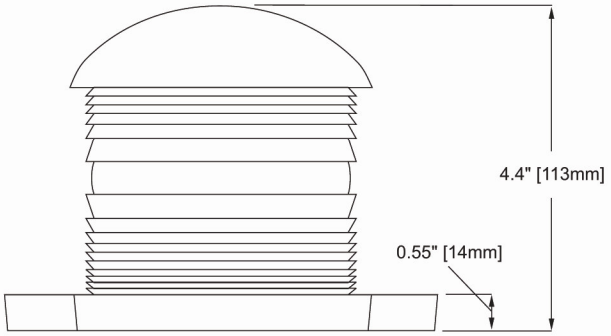

Top View

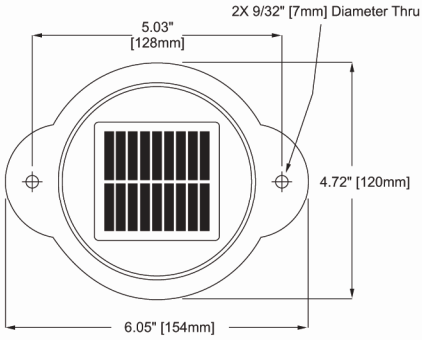

Accessories

Infrared Programmer

Security Bolt

Mounting Plate

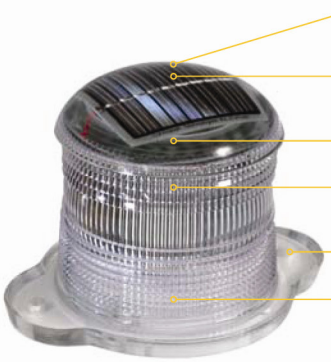

Completely self-contained
The solar panels, batteries and LEDs are brought together into one unique product.

Self-cleaning solar dome
Proprietary, dome protects solar panel while improving efficiency.

Sealed Unit
Waterproof and vandal proof.

Ultra-bright LEDs
Uses an array of bright light emitting diodes (LEDs) - no bulbs to replace, ever.

Easy to install in minutes
Using two bolts or screws.

Automatically turns on & off
On at dusk and off at dawn.

Carmanah's Model M501 solar marine lantern is a compact, light-weight and low maintenance solution for marking small buoys, docks, marinas, aquaculture weirs and other applications requiring navigation or hazard marking.

Installed in more than 110 countries, the Model M501 solar marine lantern features 1 nautical mile visibility and offers:

- **Maximum capacity with minimal life-cycle cost –** operates up to 5 years maintenance free
- **Field-proven durability –** technology tested over 15 years
- **Passed extensive shock and vibration testing**
- **IP68 certification –** tested to higher levels of water ingress protection standards
- **Vandal and theft resistant design –** high quality construction and mounting hardware
- **Patented technology –** innovative LED technology and energy management system
- **Dependable illumination –** a 10 year effective lifespan with LEDs operating up to 100,000 hours

The Model M501 is also:

- Manufactured in accordance with ISO 9001:2000 Quality Assurance Standards

Distributed by:

Premier Materials
7401 Central Ave NE
Minneapolis, MN 55432
800-262-2275
www.premiermaterials.com

[1] Transmissivity of 0.74
[2] Actual range is dependant on flash pattern, intensity, and LED color.

CE CanSIA IALA AISM RoHS IAPH

Toll Free Canada & US: 1.877.722.8877 • carmanah.com • Worldwide: +1.250.380.0052

Document: SPC_MARI-500-1NM_vE Rev. Oct 2007